STEADY-STATE TEMPERATURE RISE IN CYLINDERS WITH INTERNAL HEAT GENERATION

By

TROY JAMES PEMBERTON

Bachelor of Science
Oklahoma State University
Stillwater, Oklahoma
1962

Master of Science
Oklahoma State University
Stillwater, Oklahoma
1963

Submitted to the Faculty of the Graduate School of
the Oklahoma State University
in partial fulfillment of the requirements
for the degree of
DOCTOR OF PHILOSOPHY
August, 1965

STEADY-STATE TEMPERATURE RISE IN CYLINDERS

WITH INTERNAL HEAT GENERATION

Thesis Approved:

Gerald D. Parker
Thesis Adviser

W. A. Blackwell

Paul A. McCollum

Paul E. Torg

J. H. Boggs
Dean of the Graduate School

ACKNOWLEDGMENTS

I wish to take this opportunity to express my indebtedness to Dr. William L. Hughes for his cooperation in securing the National Defense Education Act graduate fellowship which made my entire graduate study program financially possible.

I am indebted to Professor J. D. Parker for his valuable assistance in the form of many comments, suggestions, and ideas during the course of this investigation and the writing of the thesis. His guidance and support have contributed much to the success of this part of my graduate program.

An expression of appreciation is extended to Professor William A. Blackwell, Professor Paul A. McCollum, and Professor Paul E. Long for their contributions to my entire graduate program.

In part, this work has been sponsored by the National Aeronautics and Space Administration, George C. Marshall Space Flight Center, Huntsville, Alabama, under contract numbers NAS-8-2552 and NAS-8-20052. I am grateful to Professor D. D. Lingelbach, project director, for his contributions during the course of this investigation.

I would also like to express my appreciation to my wife and family for their patience, encouragement, and sacrifice throughout the course of my collegiate studies.

TABLE OF CONTENTS

LIST OF FIGURES

CHAPTER I

INTRODUCTION

"When it smokes, it is too hot." This statement is often spoken in a facetious manner when reference is made to the temperature rating of a physical component, device, or system of components. However, the particular context from which the quotation was taken in this instance describes an unfortunate situation. In a paper presented by Rice (1) in 1962, he said, "In a corporation which does some ten billion dollars worth of business annually and has built at least 100,000,000 intermittent duty motors, the following is the sum total of all information available on armature winding temperature: 'When it smokes, it is too hot'."

There is evidence which indicates that similar statements can be made about the knowledge, or perhaps more correctly, the lack of knowledge, of the temperatures occurring within many electrical components and devices. Two possible explanations for this lack of knowledge might be as follows:

1. Temperatures occurring within electrical components are not important.
2. Temperature considerations in many applications of electrical components have simply been neglected to a large extent.

A quick glance at almost any semiconductor device specification sheet causes one to realize that temperature is a very important factor in the application of these devices. Almost without exception, the

specification sheet includes a temperature derating curve which gives an indication of the decrease in usefulness of the device as the temperature of that device increases. This indicates that the former explanation is not appropriate.

The temperature considerations have, in all likelihood, been investigated more thoroughly for semiconductor device applications than for the applications of most other electrical components and devices. This is not to say that the temperature considerations of the applications of other electrical elements is unimportant. The implication must be that there is much yet to be done in investigating the temperature problems associated with these elements. Furthermore, the conclusions drawn from these investigations must be reduced to a usable form so that proper account of the temperature characteristics of these devices can be given when considering a given device for a given application.

An excellent example of a class of components for which much work remains to be done is the group of electrical devices which include electrical coils. The electrical coil made its debut long before the science of electrical engineering became known as such. Yet, as recently as 1955, Peek and Wagar (2) said, "No rigorous treatment of heat flow in a coil is available, even for the steady-state case. The flow is 3-dimensional, the structure is not homogeneous, and the heat supply per unit length of conductor varies with local temperature. An approximate analysis in which all three of these limitations are ignored is given ...."

This thesis reports the results of an experimental and an analytical study of the temperature rise which occurs within an electrical coil when electrical power is applied to it. The temperature rise occurs

because of the joulean heat which is generated within the coil and which must be dissipated. The coil of this study is in the form of a hollow, right-circular cylinder; and only steady-state temperature rises and heat flows are considered.

More specifically, this thesis presents information that may be used in the design, analysis of design, or application study of heat-generating bodies whose geometries are described as hollow, circular cylinders. This information is derived and presented in such a manner as to provide an upper bound on the temperature rise internal to the generating body. In other words, if the given application of a cylindrical, heat-generating body comes within one of the categories of applications considered here, an equation and/or graph is presented that will give an indication of the maximum possible temperature occurring within the body.

A critique of a number of the writings which present results of studies closely related to this one is given in Chapter II. An effort is made to enumerate the more significant approximations, assumptions, and limitations of each of these works.

In Chapter III and IV a variety of boundary-value problems which are formulated to describe certain cases is considered, and the solution to each problem is presented. Some of the solutions are analytically-derived, closed-form expressions for the "hot-spot" temperature occurring within the coil, while the other solutions are obtained by solving a finite-difference model of the problem with the aid of a digital computer. The hot-spot temperature is the maximum temperature occurring within the coil.

Each boundary-value problem describes a possible application of an

electrical coil and does so by describing the temperature boundary conditions on the coil. The boundary conditions are formulated in such a way that the hot-spot temperature obtained from the solution of the boundary-value problem is an upper bound on the hot-spot temperature occurring within an actual coil whose surface temperature and heat-flow conditions closely approximate those of the problem.

The hot-spot temperature rise is the difference between the maximum temperature within the coil and the temperature at a specified point on the coil surface. The hot-spot temperature rise is of particular interest because it is at the point where this temperature occurs that the insulating material used in the coil construction will likely fail.

All of the solutions of the boundary-value problems are presented graphically in such a way as to relate the hot-spot temperature rise occurring within the coil to the power supplied to the coil and to the geometrical, electrical, and thermal properties of the coil.

The results of an experimental study are presented in Chapter V to illustrate the use of the graphs mentioned above. The coil of this study is the magnet coil of a rotary-type electromagnetic relay. The temperatures which are measured at several points on the surface of the coil are used as guides in formulating a set of temperature boundary conditions for the coil in that particular application. The resulting boundary-value problem is solved for the hot-spot temperature with the aid of a digital computer. This solution is compared with the solution of the corresponding boundary-value problem which provides an upper bound on the hot-spot temperature rise.

Chapter VI includes a restatement of the objectives of the study,

the general conclusions derived from the study, and the significant assumptions upon which those conclusions are based.

A brief description and discussion of the digital computer program and a brief error analysis are given in the appendix.

CHAPTER II

LITERATURE SURVEY

The purpose of this chapter is to present a brief summary of the recorded accounts of works which are closely associated with the work reported in this thesis pertaining to the temperature rise occurring within cylindrical heat sources. The summary consists primarily of a discussion of the class of problems for which solutions are obtained and a listing of the significant assumptions and approximations upon which these solutions are based. In every case, only the steady-state temperature distributions are considered.

In his book, Moore (3) presents a significant result which apparently has not been duplicated, mathematically verified, or extended. Based on the technique of field mapping, he derives a relationship between the thermal conductivity of the insulation on the coil wire and the combined thermal conductivity of the coil wire and insulation. This thermal conductivity is that of an "equivalent" homogeneous coil where "equivalent" implies that this coil has the same terminal characteristics as the actual coil. The results are presented graphically for both non-embedded and for embedded coils. The assumption is made that the entire space between the coil windings is filled with the insulating material. This work is referenced in several later works and will be referenced later in this thesis.

In 1943, Jakob (4) published his work pertaining to the temperature

distribution in electrical coils of "simple form" where the heat generation is nonuniform. His simple forms consist of an infinite plane plate, a solid cylinder of infinite length, and a solid sphere. The heat generation is assumed to be homogeneously distributed and to be a linear function of the temperature where the temperature coefficient is positive. The boundary conditions are simple; namely, a uniformly-distributed surface temperature. The solutions are obtained as analytical expressions which give the temperature distribution and hot-spot temperature rise above the surface temperature.

Following Jakob's work, Higgins (5) reported his work pertaining to the temperature distribution in electrical coils of general rectangular cross section. The boundary conditions are as before, a uniformly-distributed surface temperature. The heat generation is assumed to be homogeneously distributed and linearly dependent upon temperature. It is further assumed that the effects of the curvature of the coil may be neglected. That is to say, the ratio of the thickness of the coil to the inner radius is very small.

Two special cases are considered. The first is the case where the temperature coefficient of heat generation becomes zero, and the other is the case where the toroid approaches a hollow cylinder of infinite length.

In 1948 Jakob (6) reported the results of more work in the area of temperature distributions in simple bodies developing heat. In this work the heat generation is again assumed to be a linear function of the temperature, but in this case the temperature coefficient is negative. Again the body shapes are a plane infinite plate, a solid circular cylinder of infinite length, and a solid sphere.

Two cases are considered by Emmerich (7) in his work pertaining to the temperature rise in magnet coil windings. His first consideration is that of small temperature rises occurring within coils which are in the shape of right-circular, hollow cylinders. The assumptions are made that the heat generation is uniformly distributed throughout the interior, all the thermal properties of the coil are independent of temperature, and the dimensions of the coil are such that the end-effects may be neglected. The boundary conditions are (i) those of a uniformly-distributed temperature on each of the coil surfaces in one instance, and (ii) the core is thermally insulated while the outside surface is at a fixed temperature. Expressions relating the maximum temperature rise above the surface temperature (hot-spot temperature rise) and the average temperature rise to the ratio of the outer radius to the inner radius of the coil are derived analytically and presented graphically.

For the case of large temperature rises, an expression for an approximate correction to be applied to the former results is derived and presented graphically. This correction factor accounts for the error involved in assuming that the heat generation is uniformly distributed. The larger the temperature rise, the greater is the error involved; and, therefore, the greater is the correction required.

The work reported by Peek (8) is presented again by Peek and Wagar (9). This work pertains specifically to the temperature distributions in electromagnetic relay coils which are in the shape of hollow cylinders. The assumptions upon which the solutions are based are (i) the heat flow is entirely radial, (ii) the heat generated per unit volume per unit time is a constant, and (iii) the material of the coil is homogeneous and its conductivity is independent of temperature.

Expressions are derived for the hot-spot temperature rise and the average temperature rise occurring within the coil.

In summarizing this critique, the more common and pertinent assumptions and approximations that have been made in the works mentioned are presented here:

(i) The material of the coil is homogeneous and its thermal conductivity is independent of temperature.

(ii) In most cases, only radial heat flow is considered for the coil whose shape is that of a circular cylinder.

(iii) In some cases, the heat generation is considered to be uniformly distributed throughout the interior of the coil.

(iv) In nearly every case, the surface temperature condition is that of a uniformly-distributed temperature.

(v) In some cases, the effects of the curvature of the coil surfaces are neglected.

The boundary-value problems and their solutions as presented in Chapter III and IV are also based on assumptions (i) and (iii) above. However, an important difference in the results of the study presented in this thesis and those results discussed above is that no restrictions concerning axial flow of heat, effects of curvature, or end effects are made.

When these restrictions are placed upon the solutions, the effect is that of saying that the solutions are valid only for the limiting cases of (i) the length of the coil is very long compared to its thickness, and (ii) the thickness of the coil is small compared to the inner radius of the coil. These limiting cases are presented in Chapter III for a variety of temperature and heat-flow boundary conditions.

Perhaps more important, however, the solutions to the problems which fall between these limiting cases are also presented in Chapter IV. These solutions are important because they describe the usual situations.

CHAPTER III

HOT-SPOT TEMPERATURES IN HOLLOW CYLINDRICAL BODIES WITH HEAT GENERATION

Temperature Field Equation

In order to appreciate the significance and the implications of many of the assumptions that are made in the process of determining the temperature distribution in any given body, one form of the general heat-conduction equation is given here to serve as the starting point for the analysis. This is the equation

$$\frac{\partial}{\partial x}\left(k\,\frac{\partial t}{\partial x}\right) + \frac{\partial}{\partial y}\left(k\,\frac{\partial t}{\partial y}\right) + \frac{\partial}{\partial z}\left(k\,\frac{\partial t}{\partial z}\right) + q''' = \rho C\,\frac{\partial t}{\partial \theta}\,, \qquad (3.1)$$

where k, q''', C, ρ, θ, and t are thermal conductivity, heat generation per unit volume per unit time, specific heat, density, time, and temperature, respectively. The first four of these quantities may be functions of the spatial variables (x, y, z), of temperature t, and of the time θ. Also, in general the temperature t is a function of the spatial variables and of time. However, if the thermal conductivity is not a function of the spatial variables, k may be factored out of the partial derivative terms on the left-hand side of Equation 3.1 and divided out to give the equation

$$\frac{\partial^2 t}{\partial x^2} + \frac{\partial^2 t}{\partial y^2} + \frac{\partial^2 t}{\partial z^2} + \frac{q'''}{k} = \frac{1}{\alpha} \frac{\partial t}{\partial \theta} , \qquad (3.2)$$

which the temperature field $t(x,y,z,\theta)$ must satisfy. The term α is called the thermal diffusivity, a property of the conducting material and is given by

$$\alpha = k/\rho C . \qquad (3.3)$$

Continuing another step further in the simplification, if one is interested only in the steady-state temperature distribution, then the temperature field $t(x,y,z)$ must satisfy the equation

$$\frac{\partial^2 t}{\partial x^2} + \frac{\partial^2 t}{\partial y^2} + \frac{\partial^2 t}{\partial z^2} + \frac{q'''}{k} = 0 . \qquad (3.4)$$

To this point the heat generation term may still be a function of any or all of the variables (x,y,z,t). If, however, it is an explicit function of the temperature alone, then Equation 3.4 may be written as

$$\frac{\partial^2 t(x,y,z)}{\partial x^2} + \frac{\partial^2 t(x,y,z)}{\partial y^2} + \frac{\partial^2 t(x,y,z)}{\partial z^2} + \frac{q'''(t)}{k} = 0 . \qquad (3.5)$$

In general, the solutions of Equation 3.5 are more easily obtained than are the solutions of Equation 3.1. After one more simplification, Equation 3.5 takes on the form that is of particular interest in this study.

If it is assumed that the heat generation is independent of the temperature, then Equation 3.5 is reduced to the Poisson equation

$$\frac{\partial^2 t}{\partial x^2} + \frac{\partial^2 t}{\partial y^2} + \frac{\partial^2 t}{\partial z^2} + \frac{q'''}{k} = 0 \ , \qquad (3.6)$$

which must be satisfied by the temperature field t(x,y,z). This assumption is discussed later in this chapter.

In considering the temperature field within cylindrically-shaped bodies, a more appropriate form of the Poisson equation is

$$\frac{\partial^2 t}{\partial r^2} + \frac{1}{r} \cdot \frac{\partial t}{\partial r} + \frac{1}{r^2} \cdot \frac{\partial^2 t}{\partial \phi^2} + \frac{\partial^2 t}{\partial z^2} + \frac{q'''}{k} = 0 \ , \qquad (3.7)$$

where r, ϕ, and z are the cylindrical coordinates as normally defined. For the boundary-value problems under consideration in this study, it is safe to assume that the temperature field t is not a function of ϕ; therefore, t(r,z) must satisfy the equation

$$\frac{\partial^2 t}{\partial r^2} + \frac{1}{r} \cdot \frac{\partial t}{\partial r} + \frac{\partial^2 t}{\partial z^2} + a = 0 \ , \qquad (3.8)$$

where, for the sake of simplicity, $a = q'''/k$.

Dimensional Analysis

According to Hellums and Churchill (10), the objective of dimensional analysis is to reduce to a minimum the number of parameters and variables needed to describe a problem. To this end a dimensional analysis is applied to the mathematical model of interest, namely, Equation 3.8. This analysis is accomplished in the following manner.

Define the dimensionless variables

$$T = (t - t_s)/t_o \ , \ R = r/r_o \ , \ Z = z/z_o \ , \qquad (3.9)$$

where t_o, t_s, r_o, and z_o are constant parameters yet undefined, and substitute them into Equation 3.8. The result of this substitution is given as

$$\frac{t_o}{r_o^2} \cdot \frac{\partial^2 T}{\partial R^2} + \frac{t_o}{r_o^2 R} \cdot \frac{\partial T}{\partial R} + \frac{t_o}{z_o^2} \cdot \frac{\partial^2 T}{\partial Z^2} + a = 0 \ . \qquad (3.10)$$

Dividing each term of Equation 3.10 by t_o/r_o^2 yields

$$\frac{\partial^2 T}{\partial R^2} + \frac{1}{R} \cdot \frac{\partial T}{\partial R} + \frac{r_o^2}{z_o^2} \cdot \frac{\partial^2 T}{\partial Z^2} + \frac{a r_o^2}{t_o} = 0 \ . \qquad (3.11)$$

Examination of the two groups r_o^2/z_o^2 and ar_o^2/t_o shows them to be dimensionless. If each is set equal to unity and r_o is arbitrarily assigned the value r_2, the outer radius of the hollow cylinder, then the following conclusions may be drawn:

$$r_o = z_o = r_2 \ , \ t_o = a r_o^2 = a r_2^2 \ . \qquad (3.12)$$

These parameters may now be substituted back into Equation 3.11 to give

$$\frac{\partial^2 \left(\frac{t - t_s}{a r_2^2} \right)}{\partial \left(\frac{r}{r_2} \right)^2} + \frac{1}{\frac{r}{r_2}} \cdot \frac{\partial \left(\frac{t - t_s}{a r_2^2} \right)}{\partial \left(\frac{r}{r_2} \right)} + \frac{\partial^2 \left(\frac{t - t_s}{a r_2^2} \right)}{\partial \left(\frac{z}{r_2} \right)^2} + 1 = 0 \ , \qquad (3.13)$$

or more simply,

$$\frac{\partial^2 T}{\partial R^2} + \frac{1}{R} \cdot \frac{\partial T}{\partial R} + \frac{\partial^2 T}{\partial Z^2} + 1 = 0 \ , \qquad (3.14)$$

where T, R, and Z are given by Equation 3.9 and Equation 3.12.

The important conclusions concerning the necessary number of variables and parameters required to completely characterize the solution of the particular form of the heat-conduction equation of interest here can be drawn from Equation 3.14. The variables are the dimensionless ratios r/r_2, z/r_2, and $(t - t_s)/ar_2^2$. The range of variation of R and of Z is given by

$$r_1/r_2 \leq R \leq 1 \ , \ 0 \leq Z \leq L/r_2 \ , \tag{3.15}$$

where r_1 is the inner radius and L is the length of the coil. At this point, the reason for assigning the value r_2 to r_o is clear. This places a fixed maximum value of unity for R. If r_o were assigned the value r_1, then the range for R would be $(1, r_2/r_1)$ which is open ended above.

As mentioned previously, the temperature rise of greatest interest is that of the hot-spot. Since the normalized temperature rise T is a function of R and Z, it follows that the maximum value of T (T_m, the normalized hot-spot temperature rise) is a function only of the two ratios r_1/r_2 and L/r_2. This allows a graphical presentation of the relationship between T_m, r_1/r_2, and L/r_2 by plotting T_m as the dependent variable, either r_1/r_2 or L/r_2 as the independent variable and the other as a parameter.

Corresponding changes in variables must be made in the boundary conditions as were made above.

The term t_s previously undefined is the temperature at a point on the surface of the cylinder which serves as a reference point for the temperature rise determinations. More is said about t_s in the following chapter.

Uniform Heat Generation

Before proceeding further, a brief discussion to justify the assumption of uniform heat generation is given.

As mentioned in Chapter I, the purpose of this study has been to derive formulas and/or develop graphs that provide information concerning the maximum possible hot-spot temperature rise that may occur within the generating body. This is to say that the purpose is to formulate and solve boundary-value problems in such a way that the solutions will provide upper bounds on the hot-spot temperature rises occurring within actual heat-generating cylinders.

With these statements in mind, consider the following discussion:

If the electrical power supplied to the coil is obtained from a constant voltage power supply, then that power is given by

$$P = V^2/R_o\,(1 + \beta\Delta t) = P_o/(1 + \beta\Delta t) \qquad (3.16)$$

where V, R_o, β, and Δt are, respectively, the voltage applied across the coil, the resistance of coil initially, the temperature coefficient of resistance of the coil wire, and the difference in average coil temperature and the initial average coil temperature. As the temperature begins to increase after the application of the electrical power to the coil, the winding resistance increases (assuming $\beta > 0$). Since the voltage V is constant, the power P supplied to the coil must decrease as the temperature increases. The net effect of the decrease in input power is to lessen the amount of temperature increase. Therefore, the actual temperature rise is somewhat less than that calculated if the generation is assumed to be uniform ($\beta = 0$).

The result of this is that the temperature rise calculated for the case of uniform heat generation provides an upper bound on the temperature rise in the real case where the heat generation is not uniformly distributed if the electrical power is obtained from a constant voltage power supply. This case of a constant voltage supply rather than a constant current supply or a constant power supply is considered because it is felt that more often than not the electrical supply for coils in which the temperature rise is of concern more closely approximates the constant voltage supply than either of the other two.

This brief discussion brings to light a very useful observation. Even though, in its entirety, the study presented here is based on the assumption of uniform heat generation within the coil, the results derived may be extended significantly. Consider the following comments to see that this is true:

Suppose the coil of concern is energized with electrical power from a voltage regulated power supply. Also, suppose further that the temperature coefficient of resistivity of the coil wire is greater than zero (as in the case for many types of coil wire). In this situation, the heat generation is nonuniform. From Equation 3.16, the steady-state power input P to the coil is less than the initial power input P_o. The result is that the steady-state temperature rises due to an input power of P are less than the rises would be for a steady-state power input of P_o.

Therefore, the results (formulas and graphs) derived for the uniform heat generation case may be applied to the case on nonuniform generation also if the initial power input is used instead of the steady-state value.

The relative magnitudes of the temperature rise resulting from constant voltage, constant power, and constant current inputs, each with the same initial power, are shown by Peek and Wagar (11).

Formulation of Boundary-Value Problems

In a study such as the one reported here, it is desirable to consider a wide variety of cases so that the results may find a greater number of possible applications. This is to say that the results of the study should be applicable to as wide a cross section of actual electrical coil applications as is possible and within reason.

With these thoughts in mind, the collection of boundary-value problems considered is illustrated in Figure 2. Figure 1 shows a cross-sectional view of a general hollow, cylindrical coil. The regular variables and parameters are shown in Figure 1(A), and the dimensionless variables are shown in Figure 1(B).

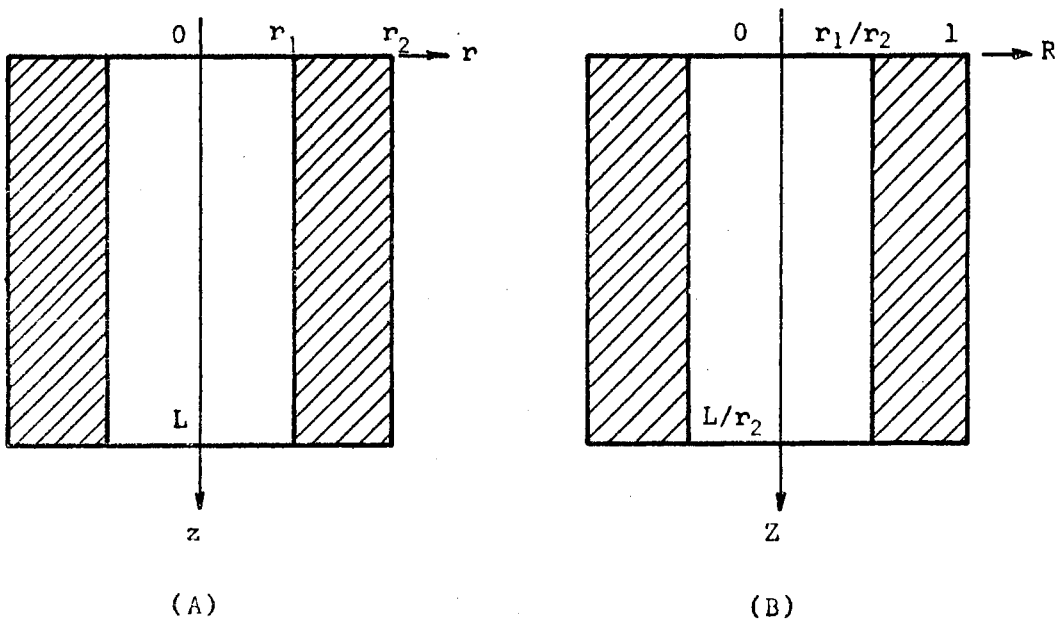

Figure 1. Cross-Sectional View of Hollow, Cylindrical Coil

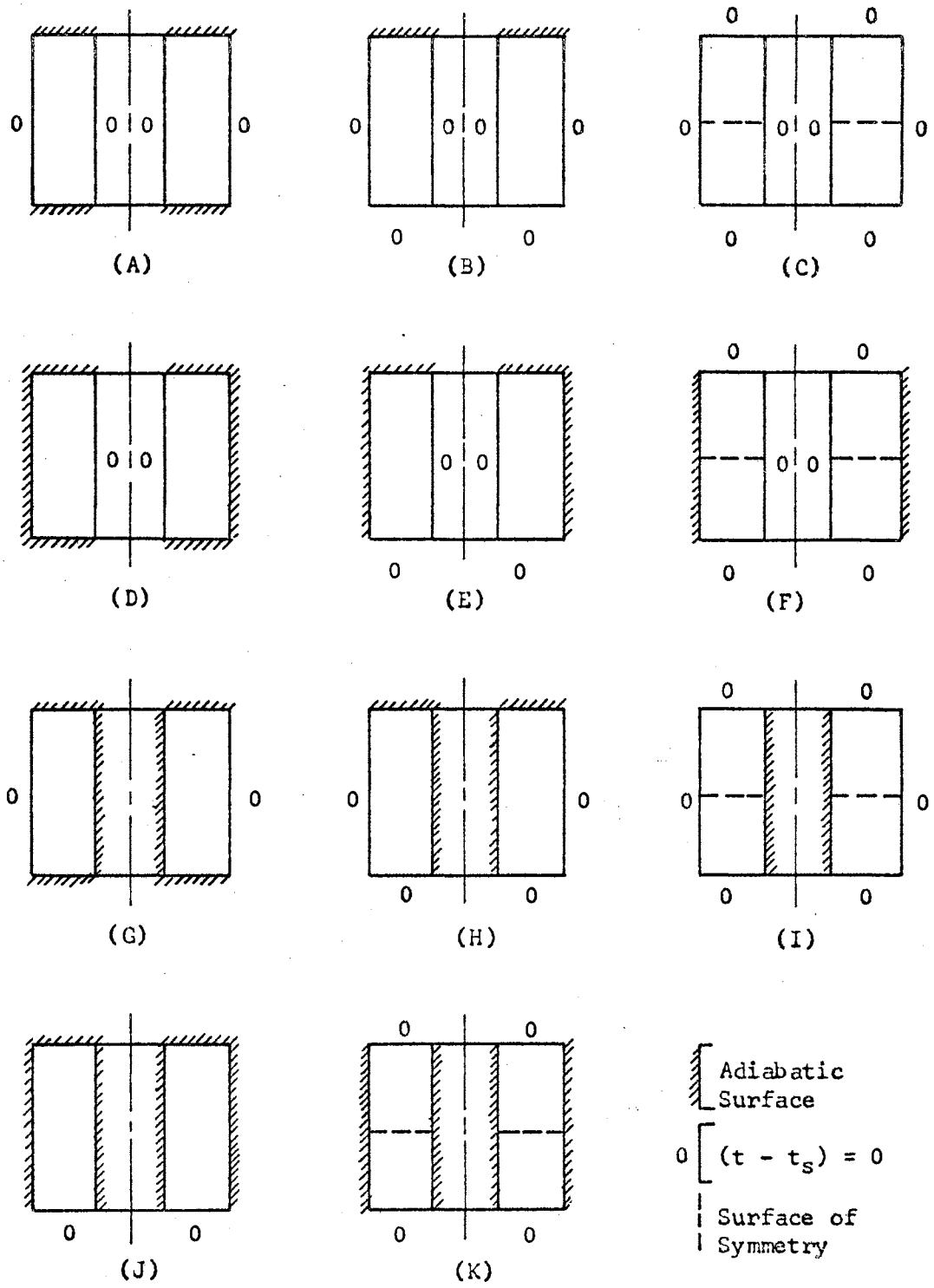

Figure 2. Illustrated List of Boundary-Value Problems

Although there most certainly are applications for cylindrical, electrical coils which result in temperature boundary conditions substantially different from any of those shown in Figure 2, it is felt that many coil applications are of such a nature that the resulting surface temperature conditions are closely approximated by one or more of the cases shown. Whenever this is true, the solution of the corresponding boundary-value problem of Figure 2 may be used to determine an upper bound on the hot-spot temperature rise occurring within the actual coil. The more closely the two sets of surface temperatures and heat flow conditions agree, the more closely the hot-spot temperature rise agrees with the calculated upper limit.

Just as intuition is valuable in most analyses of engineering problems, intuition is useful here in selecting the "best" case with which the actual case is to be compared. However, the amount of quantitative information required to use the results has been kept to a minimum by the very nature of the approach taken to predict the hot-spot temperature rise.

The mathematical description of each of the boundary-value problems shown in Figure 2 is given here and will be used subsequently in obtaining the solutions of these problems. In every case, the temperature field is independent of the angle ϕ.

Problem A:

$$T(R,Z) = 0 \qquad R = r_1/r_2 , 1 \; ; \; 0 \leq Z \leq L/r_2$$

$$\frac{\partial T(R,Z)}{\partial Z} = 0 \qquad r_1/r_2 \leq R \leq 1 \; ; \; Z = 0 , L/r_2 \tag{3.17}$$

Problem B:

$$T(R,Z) = 0 \qquad \begin{cases} R = r_1/r_2 \ , \ 1 \ ; \ 0 \leq Z \leq L/r_2 \\ r_1/r_2 \leq R \leq 1 \ ; \ Z = L/r_2 \end{cases} \tag{3.18}$$

$$\frac{\partial T(R,Z)}{\partial Z} = 0 \qquad r_1/r_2 \leq R \leq 1 \ ; \ Z = 0$$

Problem C:

$$T(R,Z) = 0 \qquad \begin{cases} R = r_1/r_2 \ , \ 1 \ ; \ 0 \leq Z \leq L/r_2 \\ r_1/r_2 \leq R \leq 1 \ ; \ Z = 0 \ , \ L/r_2 \end{cases} \tag{3.19}$$

Notice the surface of symmetry (dotted line) in Figure 2(C). This is an adiabatic surface like the top surface of Figure 2(B); and, therefore, the temperature distribution in the top half of Figure 2(C) is the mirror image of that of the bottom half. Both are identical to the distribution in the cylinder shown in Figure 2(B) if L of Equation 3.19 is the half-length of the cylinder in Figure 2(C).

Problem D:

$$T(R,Z) = 0 \qquad R = r_1/r_2 \ ; \ 0 \leq Z \leq L/r_2$$

$$\frac{\partial T(R,Z)}{\partial R} = 0 \qquad R = 1 \ ; \ 0 \leq Z \leq L/r_2 \tag{3.20}$$

$$\frac{\partial T(R,Z)}{\partial Z} = 0 \qquad r_1/r_2 \leq R \leq 1 \ ; \ Z = 0 \ , \ L/r_2$$

Problem E:

$$T(R,Z) = 0 \qquad \begin{cases} R = r_1/r_2 \ ; \ 0 \leq Z \leq L/r_2 \\ r_1/r_2 \leq R \leq 1 \ ; \ Z = L/r_2 \end{cases}$$

$$\frac{\partial T(R,Z)}{\partial R} = 0 \qquad R = 1 \; ; \; 0 \leq Z \leq L/r_2 \tag{3.21}$$

$$\frac{\partial T(R,Z)}{\partial Z} = 0 \qquad r_1/r_2 \leq R \leq 1 \; ; \; Z = 0$$

Problem F:

$$T(R,Z) = 0 \qquad \begin{cases} R = r_1/r_2 \; ; \; 0 \leq Z \leq L/r_2 \\ r_1/r_2 \leq R \leq 1 \; ; \; Z = 0 \; , \; L/r_2 \end{cases} \tag{3.22}$$

$$\frac{\partial T(R,Z)}{\partial R} = 0 \qquad R = 1 \; ; \; 0 \leq Z \leq L/r_2$$

The same comments relative to the surface of symmetry in Figure 2(F) can be made as were made about Figure 2(C).

Problem G:

$$T(R,Z) = 0 \qquad R = 1 \; ; \; 0 \leq Z \leq L/r_2$$

$$\frac{\partial T(R,Z)}{\partial R} = 0 \qquad R = r_1/r_2 \; ; \; 0 \leq Z \leq L/r_2 \tag{3.23}$$

$$\frac{\partial T(R,Z)}{\partial Z} = 0 \qquad r_1/r_2 \leq R \leq 1 \; ; \; Z = 0 \; , \; L/r_2$$

Problem H:

$$T(R,Z) = 0 \qquad \begin{cases} R = 1 \; ; \; 0 \leq Z \leq L/r_2 \\ r_1/r_2 \leq R \leq 1 \; ; \; Z = L/r_2 \end{cases}$$

$$\frac{\partial T(R,Z)}{\partial R} = 0 \qquad R = r_1/r_2 \; ; \; 0 \leq Z \leq L/r_2 \tag{3.24}$$

$$\frac{\partial T(R,Z)}{\partial Z} = 0 \qquad r_1/r_2 \leq R \leq 1 \; ; \; Z = 0$$

Problem I:

$$T(R,Z) = 0 \qquad \begin{cases} R = 1 \; ; \; 0 \leq Z \leq L/r_2 \\ r_1/r_2 \leq R \leq 1 \; ; \; Z = 0 \; , \; L/r_2 \end{cases} \tag{3.25}$$

$$\frac{\partial T(R,Z)}{\partial R} = 0 \qquad R = r_1/r_2 \; ; \; 0 \leq Z \leq L/r_2$$

Again, the same comments relative to the surface of symmetry of Figure 2(I) can be made as before.

Problem J:

$$T(R,Z) = 0 \qquad r_1/r_2 \leq R \leq 1 \; ; \; Z = L/r_2$$

$$\frac{\partial T(R,Z)}{\partial R} = 0 \qquad R = r_1/r_2 \; , \; 1 \; ; \; 0 \leq Z \leq L/r_2 \tag{3.26}$$

$$\frac{\partial T(R,Z)}{\partial Z} = 0 \qquad r_1/r_2 \leq R \leq 1 \; ; \; Z = 0$$

Problem K:

$$T(R,Z) = 0 \qquad r_1/r_2 \leq R \leq 1 \; ; \; Z = 0 \; , \; L/r_2$$

$$\frac{\partial T(R,Z)}{\partial R} = 0 \qquad R = r_1/r_2 \; , \; 1 \; ; \; 0 \leq Z \leq L/r_2 \tag{3.27}$$

Still again, the same comments relative to the surface of symmetry of Figure 2(K) can be made as before.

Examination of problems A, D, G, J, and K shows that they are

different from the rest in that the boundary conditions allow heat to flow in either the radial direction or the axial direction but not both. The implication here is that Equation 3.14 may be further simplified to an ordinary differential equation for these problems.

The general solution of each of the resulting ordinary differential equations may be obtained by applying the standard methods used to solve linear ordinary differential equations. These two equations and the corresponding general solutions are:

$$\frac{d^2T}{dR^2} + \frac{1}{R} \cdot \frac{dT}{dR} + 1 = 0 \ , \tag{3.28}$$

$$T(R) = - R^2/4 + C_1 \ln R + C_2 \ ; \tag{3.29}$$

and

$$\frac{d^2T}{dZ^2} + 1 = 0 \ , \tag{3.30}$$

$$T(Z) = - \frac{Z^2}{2} + C_1 Z + C_2 \ . \tag{3.31}$$

The problems are grouped together in Figure 2 in a certain way for a special reason. Consider the case where L/r_2 approaches infinity (or $L/r_2 >> 1$). Then problems A, B, and C all reduce to the same problem, one in which the heat flow is entirely radial (ends of coil are not considered). Under the same assumption, problems D, E, and F become identical as do problems G, H, and I, each involving only radial variations in T. For all of these cases, the differential equation of interest is Equation 3.28, and the corresponding general solution is given by Equation 3.29.

The problems J and K involve only axial heat flow, and the differential equation is Equation 3.30. The corresponding general solution is Equation 3.31.

The remainder of this chapter is devoted to the solutions of problems B, C, E, F, H, and I under the assumption that L/r_2 is very large, and of problems A, D, G, J, and K for which no assumptions concerning length are required.

Chapter IV is devoted to the solutions of problems B, C, E, F, H, and I when the length of the coil is of the same order of magnitude as the other coil dimensions.

Classical Solutions of Boundary-Value Problems for Hot-Spot Temperature Rise

As discussed previously, for the case where L/r_2 approaches infinity, the thermal models of problems A, B, and C all reduce to the same model. This model is characterized mathematically as follows. The dimensionless temperature field T(R) must satisfy the equation

$$\frac{d^2T}{dR^2} + \frac{1}{R} \cdot \frac{dT}{dR} + 1 = 0 \ , \qquad (3.28)$$

subject to the boundary conditions

$$T(R) = 0 \text{ for } R = r_1/r_2 \text{ and } 1 \ , \qquad (3.32)$$

The general solution of Equation 3.28 is stated as Equation 3.29 but is derived here. Also, the derivation of this solution may be found in most differential equation texts.

Making use of the fact that

$$\frac{d^2T}{dR^2} + \frac{1}{R} \cdot \frac{dT}{dR} = \frac{1}{R} \cdot \frac{d}{dR} \left(R \frac{dT}{dR} \right) , \tag{3.33}$$

Equation 3.28 may be written as

$$d \left(R \frac{dT}{dR} \right) = -R \, dR \tag{3.34}$$

which may be integrated to yield

$$R \frac{dT}{dR} = - \frac{R^2}{2} + C_1 . \tag{3.35}$$

Upon separating variables in Equation 3.35, the result may again be integrated to give

$$T = \int dT = \int \left(- \frac{R}{2} + \frac{C_1}{R} \right) dR = - \frac{R^2}{4} + C_1 \ln R + C_2$$

which is Equation 3.29.

From Equation 3.29 and Equation 3.32

$$T(r_1/r_2) = 0 = - \frac{(r_1/r_2)^2}{4} + C_1 \ln (r_1/r_2) + C_2 \tag{3.36a}$$

$$T(1) = 0 = - \frac{1}{4} + C_1 \ln 1 + C_2 . \tag{3.36b}$$

From Equation 3.36b, $C_2 = 1/4$, and substituting this back into Equation 3.36a yields the result

$$C_1 = \frac{(r_1/r_2)^2 - 1}{4 \ln (r_1/r_2)} .$$

For the sake of simplicity, the ratio r_1/r_2 is assigned the symbol R_{12},

$$R_{12} \equiv r_1/r_2 .$$

Now, making the substitutions for C_1 and C_2 back into Equation 3.29 gives the temperature field as

$$T(R) = - \frac{R^2}{4} + \frac{R_{12}^2 - 1}{4 \ln R_{12}} \ln R + \frac{1}{4}$$

or

$$T(R) = \frac{1}{4} \left[1 - R^2 + \frac{R_{12}^2 - 1}{\ln R_{12}} \ln R \right] . \qquad (3.37)$$

In order to find the hot-spot temperature rise, the maximum value of T(R) is found from Equation 3.37 by setting the first derivative equal to zero and solving for R_m, the value of R for which T is maximum.

$$\frac{dT(R_m)}{dR} = - \frac{R_m}{2} + \frac{R_{12}^2 - 1}{4 \ln R_{12}} \cdot \frac{1}{R_m} \qquad (3.38)$$

and

$$\frac{dT(R_m)}{dR} = 0 \Rightarrow R_m = \left[\frac{2 (R_{12}^2 - 1)}{4 \ln R_{12}} \right]^{1/2} = \left[\frac{R_{12}^2 - 1}{2 \ln R_{12}} \right]^{1/2} \qquad (3.39)$$

The desired equation for the hot-spot temperature rise is obtained now by substituting the value of R_m into Equation 3.37 to give T_m as

$$T_m = T(R_m) = \frac{1}{4} \left[1 - \left(\frac{R_{12}^2 - 1}{2 \ln R_{12}} \right) + \frac{R_{12}^2 - 1}{\ln R_{12}} \cdot \ln \left(\frac{R_{12}^2 - 1}{2 \ln R_{12}} \right)^{1/2} \right]$$

or

$$T_m = \frac{1}{4} \left[1 + \overline{R} (\ln \overline{R} - 1) \right] , \qquad (3.40)$$

where

$$\overline{R} = \frac{R_{12}^2 - 1}{2 \ln R_{12}} \quad \text{and} \quad L/r_2 >> 1 . \qquad (3.41)$$

This result, namely Equation 3.40, is the exact solution of problem A and the solution of problems B and C if L/r_2 is very large. Equation 3.40 is presented graphically in Figure 3 where T_m is plotted as a function of R_{12}. If the point at which T_m occurs is of interest, it may be found from Equation 3.39 which is presented graphically in Figure 4.

For the case where L/r_2 approaches infinity, the mathematical models of problems D, E, and F all reduce to the same model. Again, the temperature field T(R) must satisfy Equation 3.28 but subject to the boundary conditions of

$$T(R) = 0 \text{ for } R = R_{12} \ , \tag{3.42a}$$

and

$$\frac{dT(R)}{dR} = 0 \text{ for } R = 1 \ . \tag{3.42b}$$

These boundary conditions are used to determine the integration constants in Equation 3.29.

From Equations 3.29 and 3.42

$$T(R_{12}) = 0 = -\frac{R_{12}^2}{4} + C_1 \ln R_{12} + C_2 \ , \tag{3.43a}$$

and

$$\frac{dT(1)}{dR} = 0 = -\frac{1}{2} + \frac{C_1}{1} \ . \tag{3.43b}$$

Upon solving Equation 3.43 for C_1 and C_2 and substituting these back into Equation 3.29, the temperature field is determined to be

$$T(R) = -\frac{R^2}{4} + \frac{1}{2} \ln R + \frac{R_{12}^2}{4} - \frac{1}{2} \ln R_{12} \ . \tag{3.44}$$

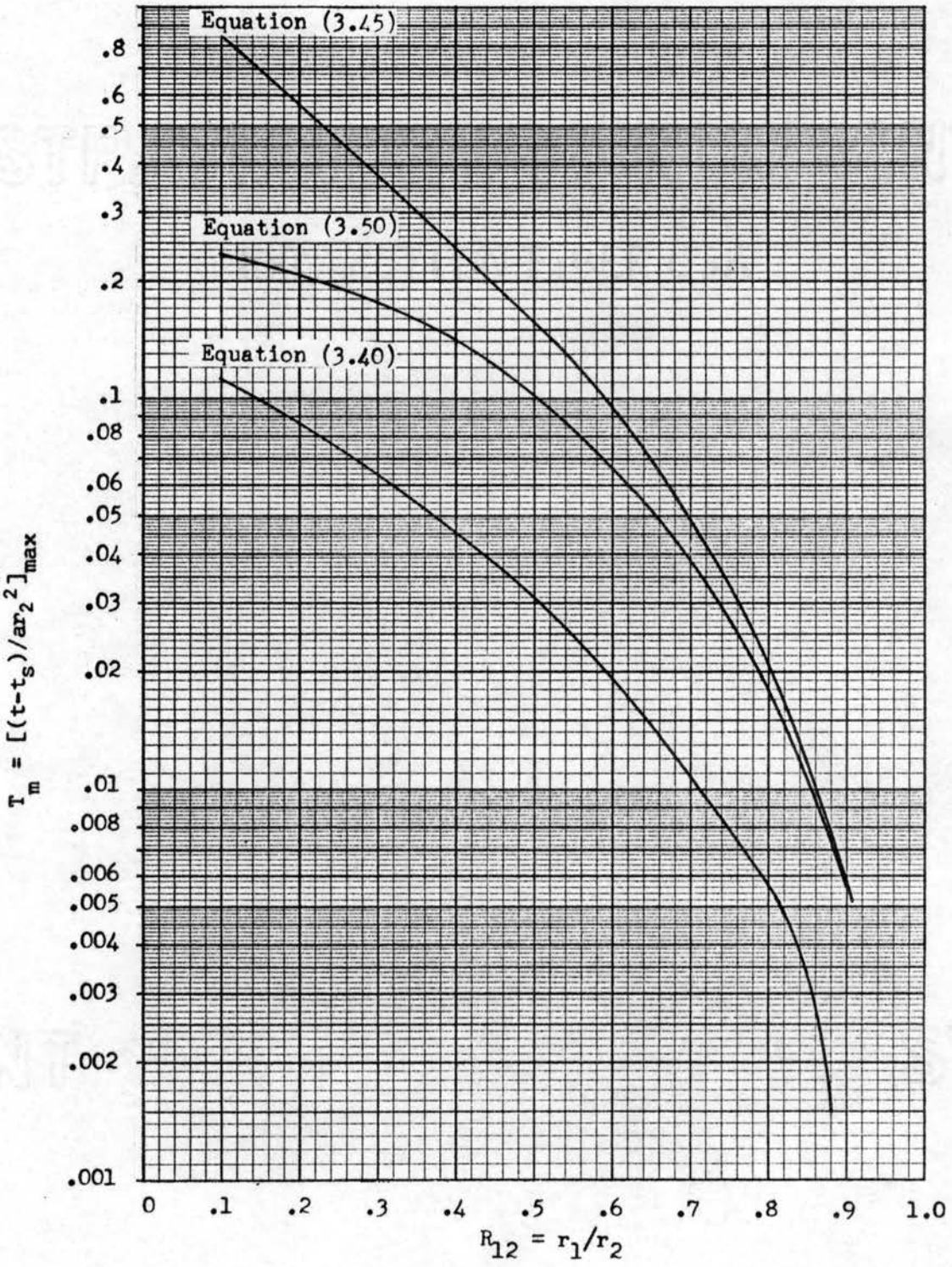

Figure 3. T_m versus R_{12} for Exact Solutions

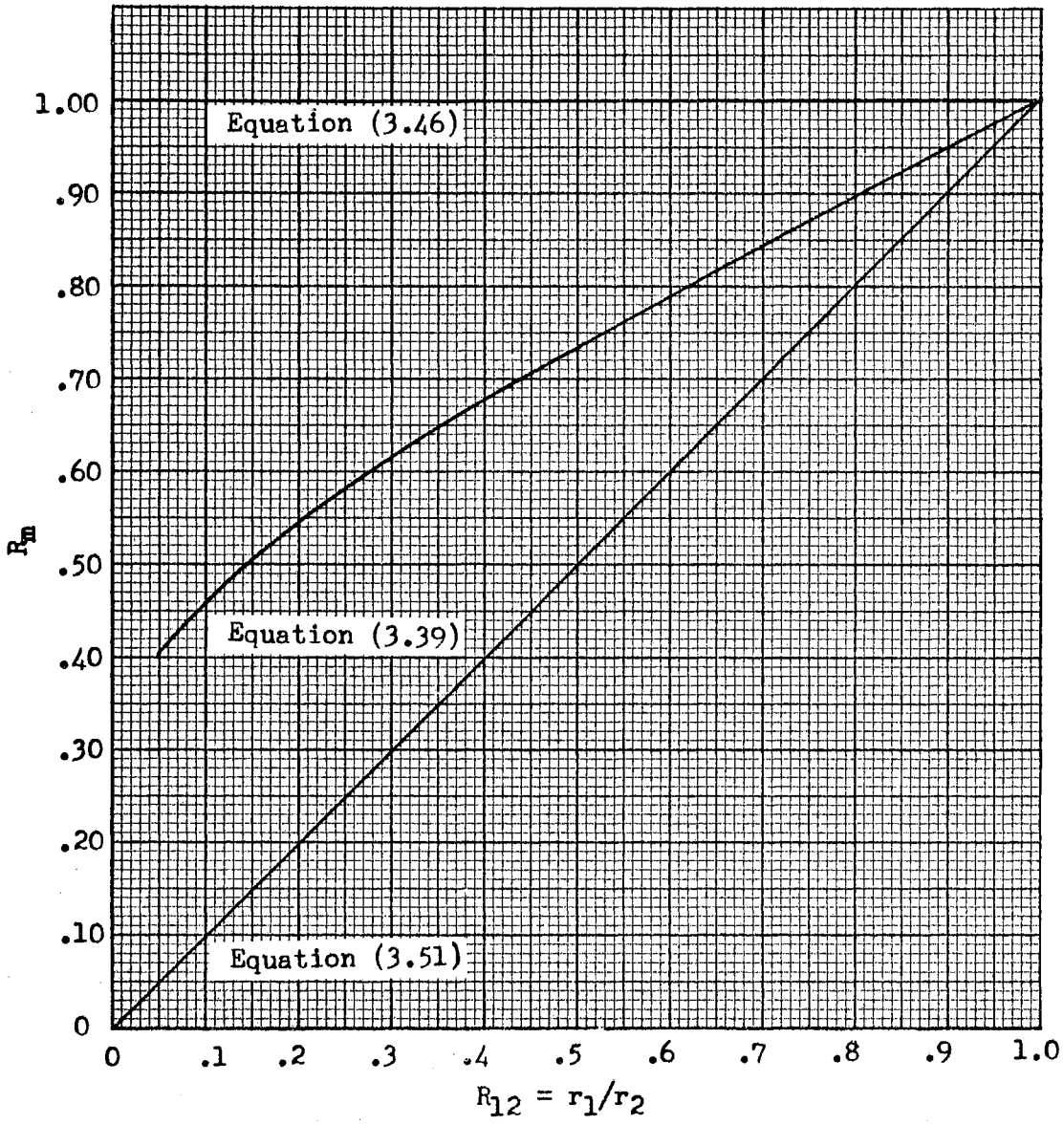

Figure 4. R_m versus R_{12} for Exact Solutions

The maximum value of T(R) from Equation 3.44 is found to be

$$T_m = T(1) = \frac{1}{4}(R_{12}^2 - 1) - \frac{1}{2} \ln R_{12}^2 \ , \qquad (3.45)$$

and R_m is seen to be

$$R_m = 1 \ . \qquad (3.46)$$

Equation 3.45 is also presented graphically in Figure 3 and Equation 3.46 in Figure 4. Just as before, Equation 3.45 is the exact solution to problem D and is an approximate solution to problems E and F, where the error of the approximation decreases as L/r_2 increases.

A mathematical model similar to the ones used in the previous two solutions may be used for problems G, H, and I. Again, the temperature field must satisfy Equation 3.29 where the boundary conditions in this case are

$$\frac{dT(R)}{dR} = 0 \text{ for } R = R_{12} \ , \qquad (3.47a)$$

and

$$T(R) = 0 \text{ for } R = 1 \ . \qquad (3.47b)$$

From Equations 3.29 and 3.47

$$T(1) = 0 = -\frac{1}{4} + C_1 \ln 1 + C_2 \ , \qquad (3.48a)$$

and

$$\frac{dT(R_{12})}{dR} = 0 = -\frac{R_{12}}{2} + \frac{C_1}{R_{12}} \ . \qquad (3.48b)$$

The results of the simultaneous solution of Equations 3.48 for C_1 and

C_2, upon being substituted into Equation 3.29, determine the temperature field to be

$$T(R) = \frac{1}{4}(1 - R^2) + \frac{1}{2} R_{12}^2 \ln R \,. \tag{3.49}$$

The maximum value of T(R) is

$$T_m = T(R_m) = \frac{1}{4}(1 - R_{12}^2) + \frac{1}{2} R_{12}^2 \ln R_{12} \,, \tag{3.50}$$

where

$$R_m = R_{12} \,. \tag{3.51}$$

Equation 3.50 is presented graphically in Figure 3, also, in order that the hot-spot temperature rises of the first three groups of problems in Figure 2 may be easily compared. Also, Equation 3.51 is shown in Figure 4. Just as is true in the previous two solutions, Equation 3.50 is a valid solution of problems H and I only if L/r_2 is very large.

In Chapter IV, it is shown that each of the Equations 3.40, 3.45, and 3.50 is a limiting curve in a family of curves where the family parameter is L/r_2.

The two problems of Figure 2 yet to be treated are different from the problems presented thus far. The boundary conditions on these two problems, namely problems J and K, are such that the heat flow is entirely axial. The mathematical model of these problems is given as Equation 3.30 and the appropriate boundary conditions, where the general solution for the temperature field is given by Equation 3.31. Equation 3.31 is derived from Equation 3.30 here as follows:

$$\frac{d^2T}{dZ^2} = \frac{d}{dZ}\left(\frac{dT}{dZ}\right) = -1 \,. \tag{3.30}$$

This equation may be integrated by separating the variables to yield

$$\frac{dT}{dZ} = - Z + C_1 \text{ .}$$

Again, by separating the variables, the equation may be integrated to give

$$T = - \frac{Z^2}{2} + C_1 Z + C_2 \text{ ,}$$

which is precisely Equation 3.31.

Due to the line of symmetry in problem K, each half of which is identical to problem J, only problem J needs to be solved. The complete mathematical model of the thermal model shown in Figure 2(J) is

$$\frac{d^2T}{dZ^2} + 1 = 0 \text{ ,} \qquad (3.30)$$

$$\frac{dT}{dZ} = 0 \text{ for } Z = 0 \text{ ,} \qquad (3.52a)$$

and

$$T = 0 \text{ for } Z = L/r_2 \text{ .} \qquad (3.52b)$$

In order to determine the constants of integration in Equation 3.31, the following two equations are solved simultaneously:

$$\frac{dT(0)}{dZ} = 0 = C_1 \qquad (3.53a)$$

and

$$T(L/r_2) = 0 = - \frac{(L/r_2)^2}{2} + C_2 . \qquad (3.53b)$$

Substituting the values for C_1 and C_2 into Equation 3.31 yields the temperature field:

$$T(Z) = -\frac{Z^2}{2} + \frac{(L/r_2)^2}{2} \quad . \tag{3.54}$$

The hot-spot temperature rise is easily seen to be

$$T_m = T(Z_m) = T(0) = \frac{(L/r_2)^2}{2} \quad . \tag{3.55}$$

Equation 3.55 is presented graphically in Figure 5.

If the problem of interest is the one shown in Figure 2(K), then Equation 3.55 may still be used, but the L of Equation 3.55 is the half-length of the cylinder, and T_m will occur at the mid-length of the hollow cylinder.

In summary, Equations 3.40, 3.45, and 3.50 are exact solutions for the hot-spot temperatures of the thermal models of Figures 2(A), 2(D), and 2(G), and are approximate solutions of the thermal models of Figures 2(B) and 2(C), 2(E) and 2(F), and 2(H) and 2(I), respectively, if L/r_2 is much greater than unity.

The next chapter is devoted to the development of a general mathematical model for the boundary-value problems illustrated in Figure 2 and described by Equations 3.17 through 3.27. The solution of the model is accomplished by employing the techniques of finite-differences. The information given in Figure 3 is included later in Figures 9, 10, and 11 to provide a more complete solution to the group of problems of Figure 2. The entire objective of this effort is to remove the restriction of L/r_2 being very large from the solutions.

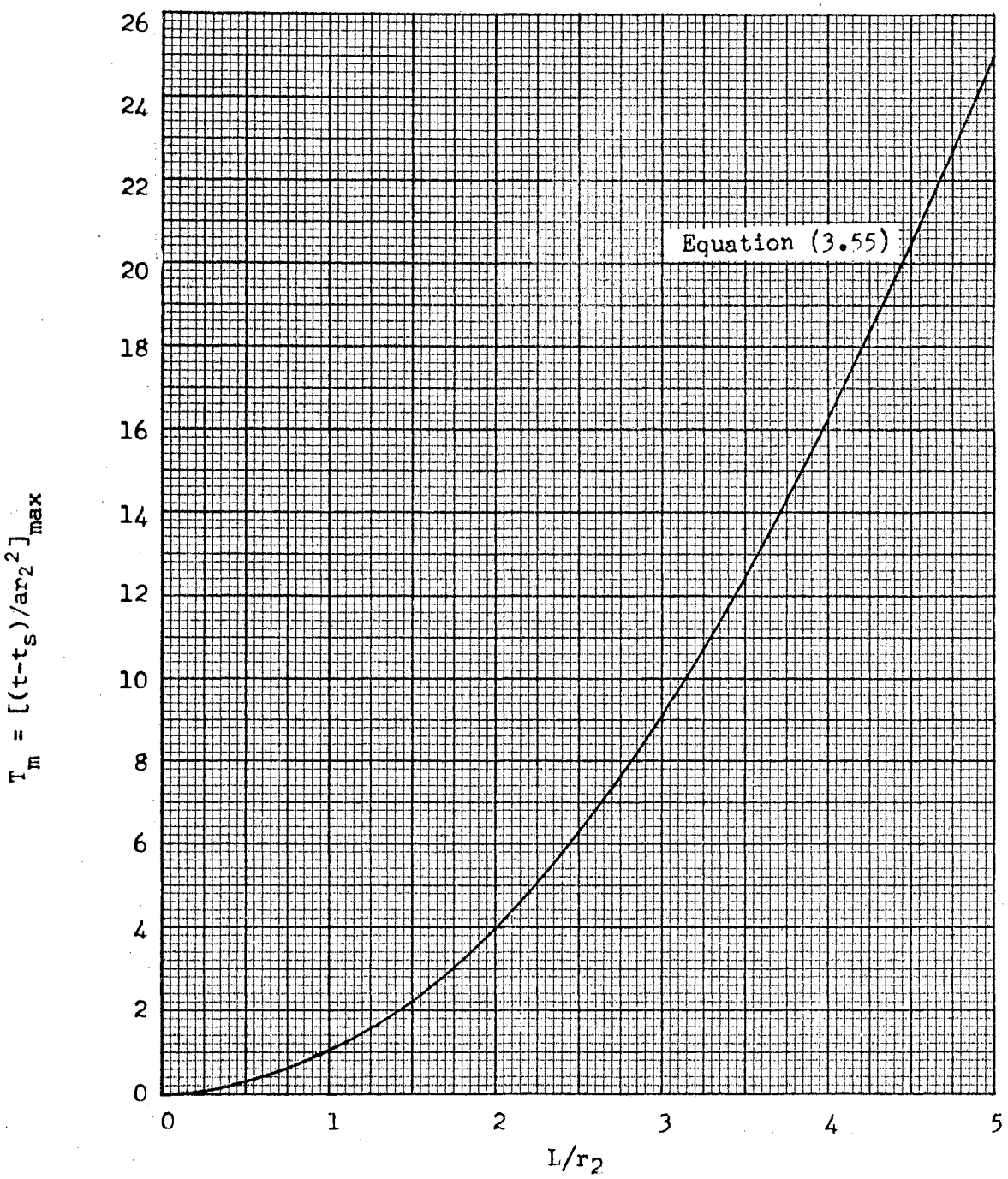

Figure 5. T_m versus L/r_2 for Purely Axial Heat Flow

CHAPTER IV

NUMERICAL SOLUTIONS OF THE BOUNDARY-VALUE PROBLEMS

In keeping with the desire to derive and present the solutions of the group of boundary-value problems shown in Figure 2 in such a way that those solutions are readily usable by the engineer, an alternate approach to the mathematics involved is taken at this point.

In Chapter III the only solutions derived are for those problems where the heat-conduction equation reduces to an ordinary differential equation. In every instance this reduction of the partial differential equation to an ordinary differential equation is a result of the boundary conditions involved or the assumptions that are made regarding the dimensions, one relative to another. For those cases where the dimensions of the coil are such that the assumption that L/r_2 is very large cannot be made, this simplification of the heat-conduction equation, namely Equation 3.14, to either Equations 3.28 or 3.30 cannot be made.

There are several approaches that may be taken to derive the solution of Equation 3.14 when subjected to boundary conditions which involve two variables. Thinking ahead just a bit, one realizes that the solution to Equation 3.14, subject to each set of boundary conditions of interest, must be determined for a range of values of R_{12} and for a range of values of L/r_2 for each value of R_{12}. If each problem is to be solved many times, it seems reasonable to consider the possibility

of using a computer in deriving the many solutions.

Either the analog or the digital computer may be used to solve partial differential equations. Through the use of certain of the numerical methods, the digital computer lends itself more directly to the solutions of those types of problems than does the analog computer. For this reason, the remainder of the solutions presented here are derived with the aid of a digital computer. A brief discussion relating to the numerical methods used and the resulting mathematical models is given here.

The numerical method of interest is that of the finite-difference approximation to the partial derivative terms of the Poisson equation (3.14). There is a number of texts which treat this subject very adequately. Three such books are those by Schneider (12) and Dusinberre (13, 14). The various aspects of these techniques are not developed here, but instead, the application of the techniques to the problems at hand.

Consider the entire volume of the heat-generating body to be divided into subvolumes, each of some specific geometrical description. Consider further that all the mass and the thermal and electrical properties of each subvolume are associated with a specific point (referred to as a node) within the subvolume. This is illustrated in Figure 6. Each node is thought to be connected to every adjacent node by a thermally-conducting rod. The conductance of each rod is determined by the separation distance between the two nodes, the thermal conductivity of the medium, the cross-sectional area between the subvolumes with which the nodes are associated, and the geometry of the subvolumes.

Making application of the finite-difference approximations, the

total heat flow into node 1 of Figure 6 is given as

$$Q_{g_1} + K_{21}(T_2 - T_1) + K_{31}(T_3 - T_1) + K_{41}(T_4 - T_1) + K_{51}(T_5 - T_1) = 0 \ , \qquad (4.1)$$

where Q_{g_1} is the heat generated in the subvolume associated with node 1, K_{j1} is the conductance from node j to node 1, and T_j is the temperature of node j.

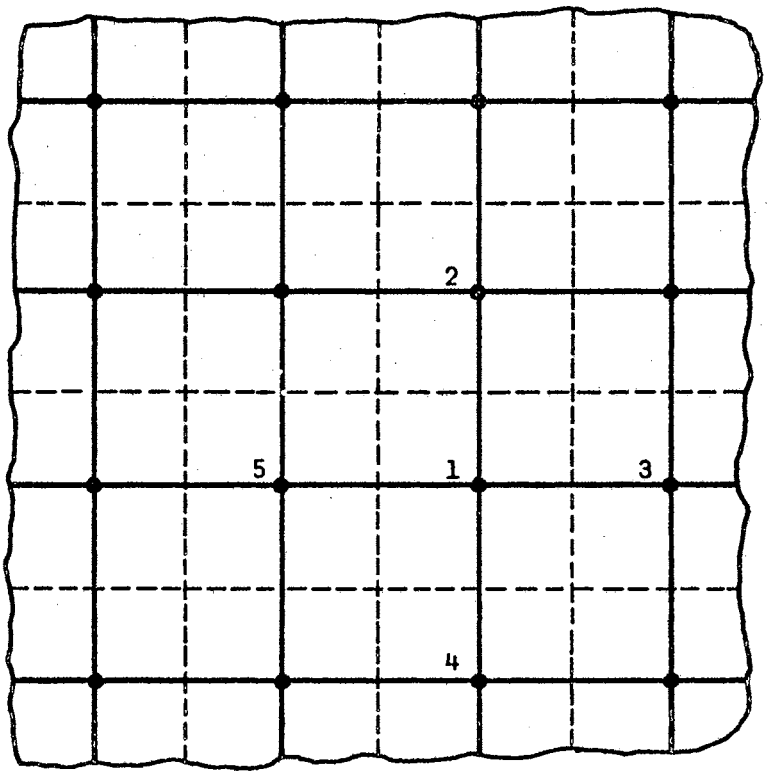

Figure 6. Finite-Difference Model

The heat generation term Q_{g_1} of Equation 4.1 may be written as the product of a thermal conductance and a temperature difference as

$$Q_{g_1} = K_{g_1}(T_{g_1} - T_1) \ . \qquad (4.2)$$

The quantity Q_{g1} is determined by dividing the total power input to the coil by the volume associated with node 1. In keeping with the assumption that the heat generation within the coil is independent of the local temperature, the temperature T_{g1} is arbitrarily specified such that

$$T_{g1} >>> T_1 \quad .$$

For practical purposes, Equation 4.2 then reduces to

$$Q_{g1} = K_{g1} T_{g1}$$

or

$$K_{g1} = Q_{g1}/T_{g1} \quad . \tag{4.3}$$

Therefore, the heat generation corresponding to node 1 may be thought of as a conductance of heat from a node of very high temperature T_{g1} to node 1 by way of a thermal conductance K_{g1}, where K_{g1} is defined by Equation 4.3.

As a result of these, Equation 4.1 may be written in the form

$$T_1 = \frac{K_{g1} T_{g1} + \sum_{j=2}^{5} K_{j1} T_j}{\sum_{j=2}^{5} K_{j1}} \tag{4.4}$$

In exactly the same manner, equations may be written for the temperature of every node in the volume. This results in a system of linear, algebraic equations to be solved simultaneously.

The system of equations of which Equation 4.4 is one may be solved in a rather straightforward manner using a digital computer.

The node array which is used in solving for the temperature field

in the cylindrical body is presented along with formulas for the conductances from one node to another.

Consider an enlarged view of the cross section of the hollow, cylindrical body shown in Figure 1(B) as now shown in Figure 7. By the very nature of each of the boundary-value problems, there is no need for the node array to extend in the azimuthal direction because the boundary conditions are such that there is no azimuthal variation in the temperature field. Therefore, the subvolume associated with each node is a toroid of rectangular cross section as illustrated in Figure 8.

The conductance from node i to node i + 1 of Figure 7 is given by

$$K_{i,i+1} = \frac{2\pi k \Delta L}{\ln (\rho_3/\rho_2)} \tag{4.5}$$

and from node j to node j + 1 by

$$K_{j,j+1} = \pi[(\rho_3 + \frac{\Delta R}{2})^2 - (\rho_3 - \frac{\Delta R}{2})^2]\, k/\Delta L$$

or

$$K_{j,j+1} = \pi k[2\rho_3 \Delta R]/\Delta L \ , \tag{4.6}$$

where k is the thermal conductivity of the medium. For the node array shown

$$\Delta R = (1 - R_{12})/6 \ ,$$

$$\Delta L = (L/r_2)/6 \ , \tag{4.7}$$

$$\rho_{i+1} = \rho_i + \Delta R \ , \ i = 1, 2, 3, 4, 5, 6$$

and

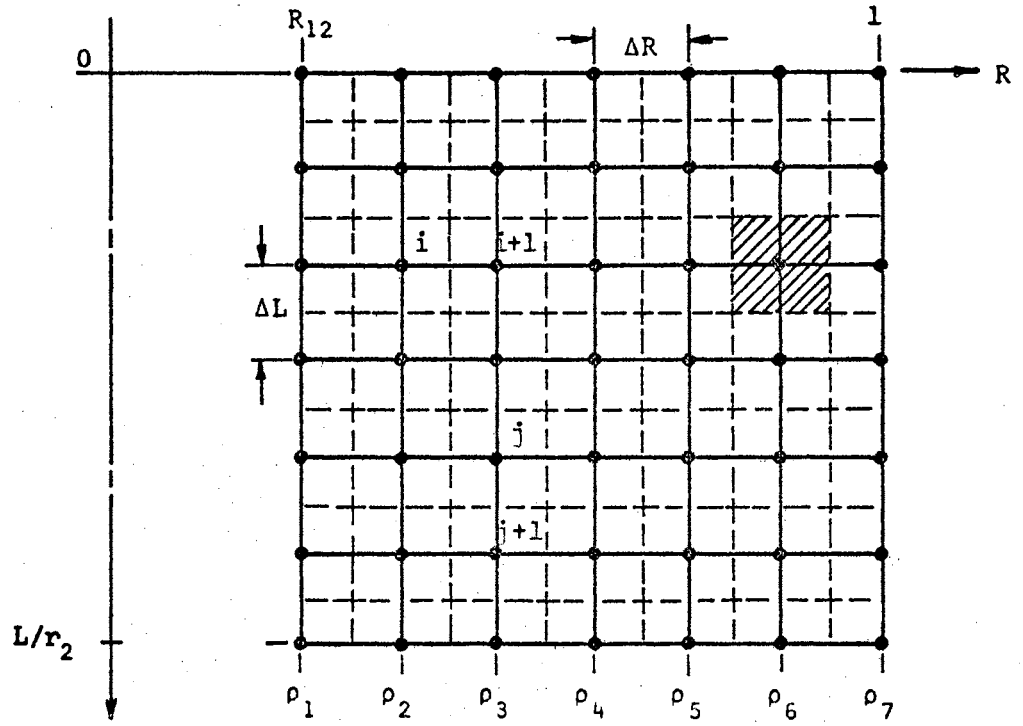

Figure 7. Node Array for Cylindrical Body

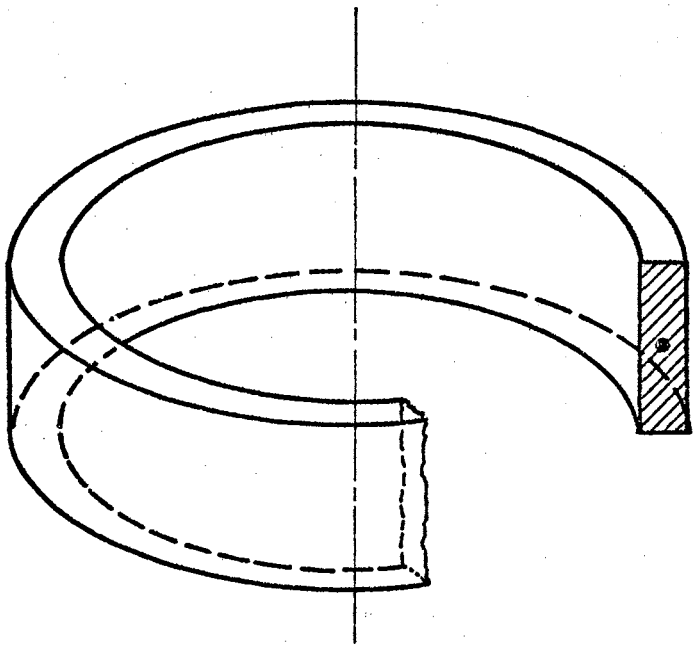

Figure 8. Toroidal Subvolume Associated with Each Node

$$\rho_1 = R_{12} .$$

A digital computer program has been developed that will calculate all of the internal thermal conductances from one node to another, calculate the heat generated within each subvolume, then formulate and solve the system of linear, algebraic equations described above for any given value of R_{12} and L/r_2. This program allows the use of any type of temperature boundary condition or adiabatic surface over any portion of the coil surface. With a small addition, the program will also allow the use of either convective or radiative surface conditions. The solution of the set of equations is accomplished by an iterative process. A description of the program is provided in Appendix A.

Because the numerical solution is only an approximate solution, there is an error involved in each of the solutions obtained by using the numerical techniques. An error analysis of the numerical solutions is provided in Appendix B. The approach taken in the analysis is to select one of the boundary-value problems that has been solved exactly by direct integration. The same problem is solved with the computer program, and results are then compared. This gives an indication of the error due to the finite-difference approximation and to the round-off occurring within the computation at the same time.

Once the computer program has been written and checked out, the solutions to the several boundary-value problems shown in Figure 2 are obtained only after numerous executions of the program. For each boundary-value problem, a set of data describing those particular boundary conditions of interest and values for R_{12} and L/r_2 must be provided.

As will be pointed out later, for all practical purposes, the value L/r_2 greater than four satisfies the restriction of L/r_2 being much greater than one for the problems of interest here. In other words, if L/r_2 is greater than four, the value of the hot-spot temperature rise is, for practical purposes, the same as the value obtained by considering the case where L/r_2 approaches infinity. This is not surprising if one compares the area of the curved surfaces to that of the ends. In the extreme case where r_1 becomes zero, the ratio of the curved surface area to the end area is

$$\frac{2\pi r_2 L}{2\pi r_2^2} = \frac{L}{r_2} \geq 4 .$$

Therefore, there is four times as much area to dissipate the heat from the curved surface as there is from the ends. As r_1 approaches r_2, this ratio becomes even greater as is easily seen from

$$\frac{2\pi r_2 L}{2\pi(r_2^2 - r_1^2)} = \frac{L}{r_2(1 - r_1^2/r_2^2)} = \frac{L/r_2}{1 - r_1^2/r_2^2} .$$

In fact, as r_1 approaches r_2, the ratio becomes infinite. As more of the heat is dissipated from the curved surfaces, the heat flow internal to the generating body becomes more radial, more dependent upon the radial parameters, and less dependent upon the axial parameters.

Selection of a Reference Temperature

In order to be assured that the hot-spot temperature rise determined from the solution of one of the boundary-value problems is an upper bound on the hot-spot temperature rise occurring within an actual coil,

some attention must be given to the selection of the proper temperature to be used as a reference.

The success of determining an upper bound on the hot-spot temperature rise within an actual coil subjected to a particular environment depends largely upon the selection of the most appropriate thermal model from the group given in Figure 2. The first step is to determine which of the coil surfaces are adiabatic or approximately so. Often this may be done by simply inspecting the coil in its operating environment and observing the possible paths for heat conduction out of and away from the coil. In many instances there may be no favorable conditions for the transfer of heat from one surface while a very good conduction path is present for heat transfer away from some other surface. Once the adiabatic surfaces have been sought out, the thermal model which has corresponding adiabatic surfaces is selected from Figure 2. The solution of this model provides the upper bound on the hot-spot temperature rise in the actual coil.

After the proper thermal model has been selected, the location of the reference temperature must be determined. The reference temperature is taken to be the maximum temperature occurring on any of the non-adiabatic surfaces. Again, by observation of the heat flow paths in a particular coil application, the location of this point is often easily approximated. It seems reasonable to assume that this temperature might often occur at the points of intersection of one of the adiabatic surfaces with one of the non-adiabatic surfaces. However, regardless of the manner in which this point is found, the temperature at that point is taken to be the reference temperature, namely, t_s as first introduced in Equation 3.9. In the thermal model which is used to provide an upper bound on the hot-spot temperature rise, the temperature

of the non-adiabatic surfaces is t_s as specified above. With this temperature uniformly distributed on all the non-adiabatic surfaces, the dimensionless temperature as defined by Equation 3.9 and Equation 3.12 is zero everywhere on those surfaces of the model.

To show that the solution of this model does provide an upper bound, consider the following comments.

Suppose that the temperature distribution on all of the non-adiabatic surfaces is a uniformly-distributed temperature t_1. Corresponding to these boundary conditions, the temperature distribution within the coil is $t(r, z)_1$, and the hot-spot temperature is t_{m1}. If the temperature t_1 is decreased to some lesser value t_2, the internal temperature distribution is $t(r, z)_2$ with a hot-spot temperature of t_{m2}. Since it has been assumed that the thermal characteristics of the coil are all temperature independent, $t(r, z)_1$, $t(r, z)_2$, t_{m1}, and t_{m2} are related in the following manner:

$$t(r,z)_1 = t(r,z)_2 + (t_1 - t_2) > t(r,z)_2$$

and

$$t_{m1} = t_{m2} + (t_1 - t_2) > t_{m2} \quad .$$

Therefore, a decrease in the temperature of the non-adiabatic surfaces of the model produces a corresponding decrease in the entire temperature distribution and hence the hot-spot temperature within the model.

Let the uniform surface temperature t_1 be replaced with a non-uniform surface distribution $t(r, z)_{surf}$ which is continuous on each of the non-adiabatic surfaces and has a maximum value t_1. The corresponding internal distribution is $t(r, z)_3$ with a hot-spot temperature

t_{m3}. Since t_1 is an upper bound on $t(r, z)_{surf}$ for all values of (r, z) on the non-adiabatic surfaces, it follows that $t(r, z)_1$ is an upper bound on $t(r, z)_3$ at every point (r, z) in the interior. This implies that t_{m1} is an upper bound on t_{m3} which is the desired conclusion. Therefore, if the maximum value of the temperature occurring on the non-adiabatic surface is taken as a reference (that is, $t_s = t_1$), the hot-spot temperature rise for the case of a uniform surface temperature is related to the hot-spot temperature rise for the case of a non-uniform temperature in the manner

$$t_{m1} - t_s \geq t_{m3} - t_s$$

or

$$T_{m1} \geq T_{m3} \quad .$$

Hence, the solution of the proper model as described in Figure 2 provides an upper bound on the hot-spot temperature rise within an energized coil when the reference temperature t_s is selected as described above.

Using completely analogous statements, it is easily seen that if the reference temperature is selected to be the minimum temperature occurring on the non-adiabatic surfaces, then the result is a lower bound on the actual hot-spot temperature rise. Just as easily seen is that the difference between the upper and the lower bound is equal to the difference between the maximum and the minimum temperatures occurring on the non-adiabatic surfaces of the coil.

In summarizing the comments pertaining to the selection of the reference temperature, it may be said that the process is carried out

by determining which surfaces of the coil are adiabatic or approximately so and where the maximum temperature occurs on the non-adiabatic portions of the coil surface. Both of these steps may possibly be accomplished in a heuristic manner or by a detailed study of the actual boundary conditions.

With these thoughts in mind, the solutions to the group of boundary-value problems as obtained with the aid of the digital computing facilities are presented and discussed.

Solution of the Boundary-Value Problems with Realistic Dimensions

As was pointed out in Chapter III, the problems shown in Figure 2(A), (D), (G), (J), and (K) may be solved by the direct integration of the appropriate ordinary differential equation and by matching two boundary conditions. Also, it was pointed out that the problems shown in Figure 2(C), (F), and (I) are simply two of the problems shown in Figure 2(B), (E), and (H), respectively, placed end to end. This comes about because lines or surfaces of symmetry are adiabatic surfaces if the boundary conditions are also symmetrical about those same lines or surfaces. Therefore, the problems of Figure 2(B), (E), and (F) must be solved for the cases where it is not permissible to assume that L/r_2 is much greater than one. Once the solution for the hot-spot temperature rise in each of these problems is obtained, the entire group of problems will have been covered.

The boundary conditions shown in Figure 2(B) and described mathematically in Equation 3.18 are used as data for the computer program. This boundary-value problem is solved for a range of values of R_{12} and

L/r_2. Figure 9 shows this solution for the dimensionless hot-spot temperature rise T_m plotted as a function of R_{12} with a parameter L/r_2. This same family of curves may be used to determine the hot-spot temperature rise in problem C as discussed previously.

It is interesting to note that if L/r_2 is greater than one, the hot-spot temperature rise is very close to that of an infinitely long coil. Just as one would expect, as R_{12} increases toward unity, the effects of length become less and less significant until, finally, the effect is less than the error involved in the numerical solution. The top curve shown in Figure 9 is the same as the bottom curve in Figure 3. This is Equation 3.40. This is also the solution to problem A.

Figure 10 shows the results from the computer solution of the problem shown in Figure 2(E). As discussed previously, this family of curves may be used to determine the hot-spot temperature of problem F, also. One notices here that the effects of length are more significant than is the case in Figure 9. This is not surprising, because the larger of the two curved surfaces has no heat flowing across it. Therefore, an increased fraction of the total heat flow must be out the end. The top curve in this figure is Equation 3.45 which is also given in Figure 3. Also, this is the solution of problem D.

Finally, Figure 11 shows the relationship between the dimensionless hot-spot temperature rise and R_{12} and L/r_2 for the boundary conditions shown in Figure 2(H). In this instance the hot-spot temperature rise is less dependent upon length than in the last problem, because heat flows across the larger of the two curved surfaces. Therefore, more heat flows radially and less axially than before. Here again, this family of curves may be used for problem I. The top curve is the same

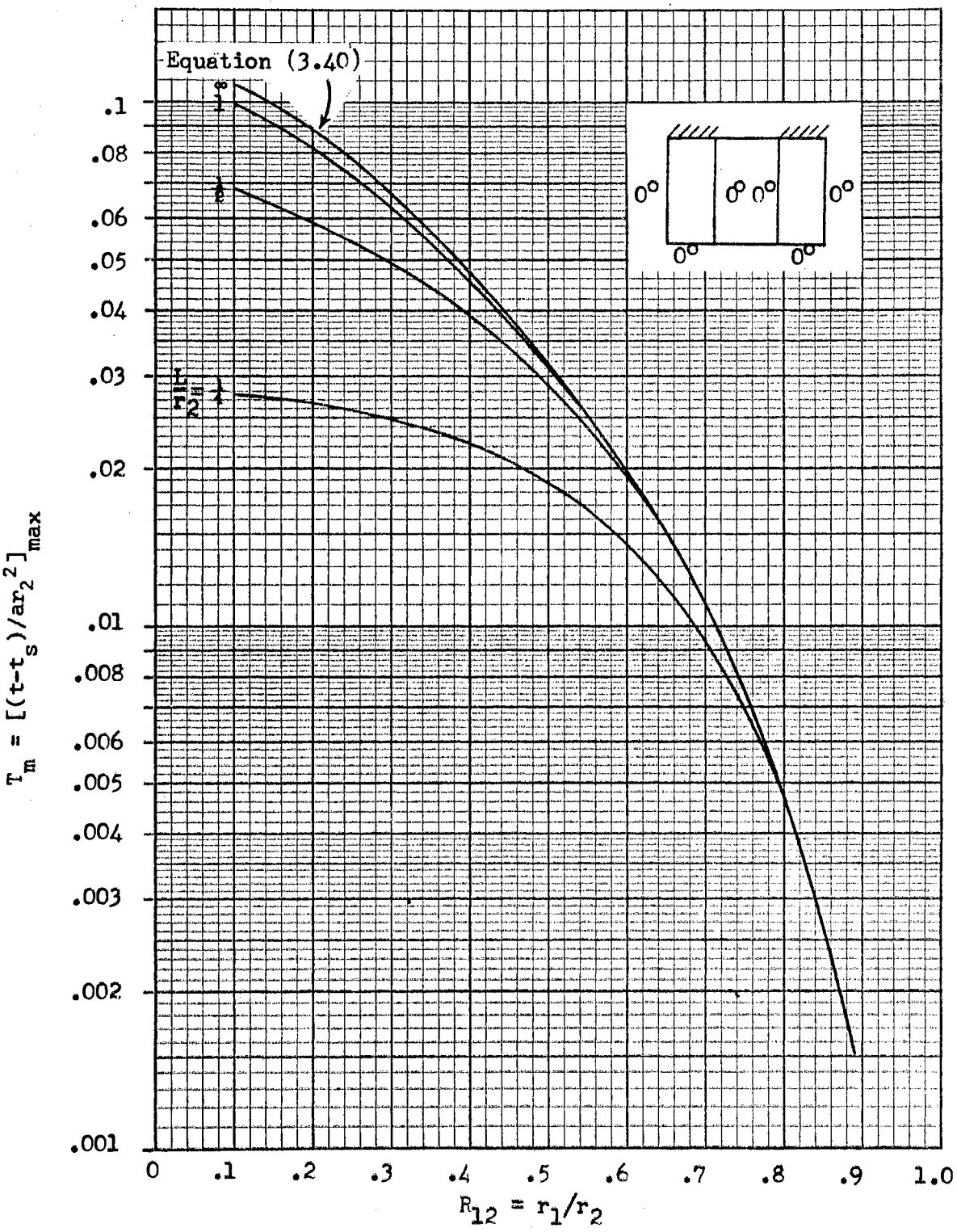

Figure 9. T_m versus R_{12} for Problems A,B, and C

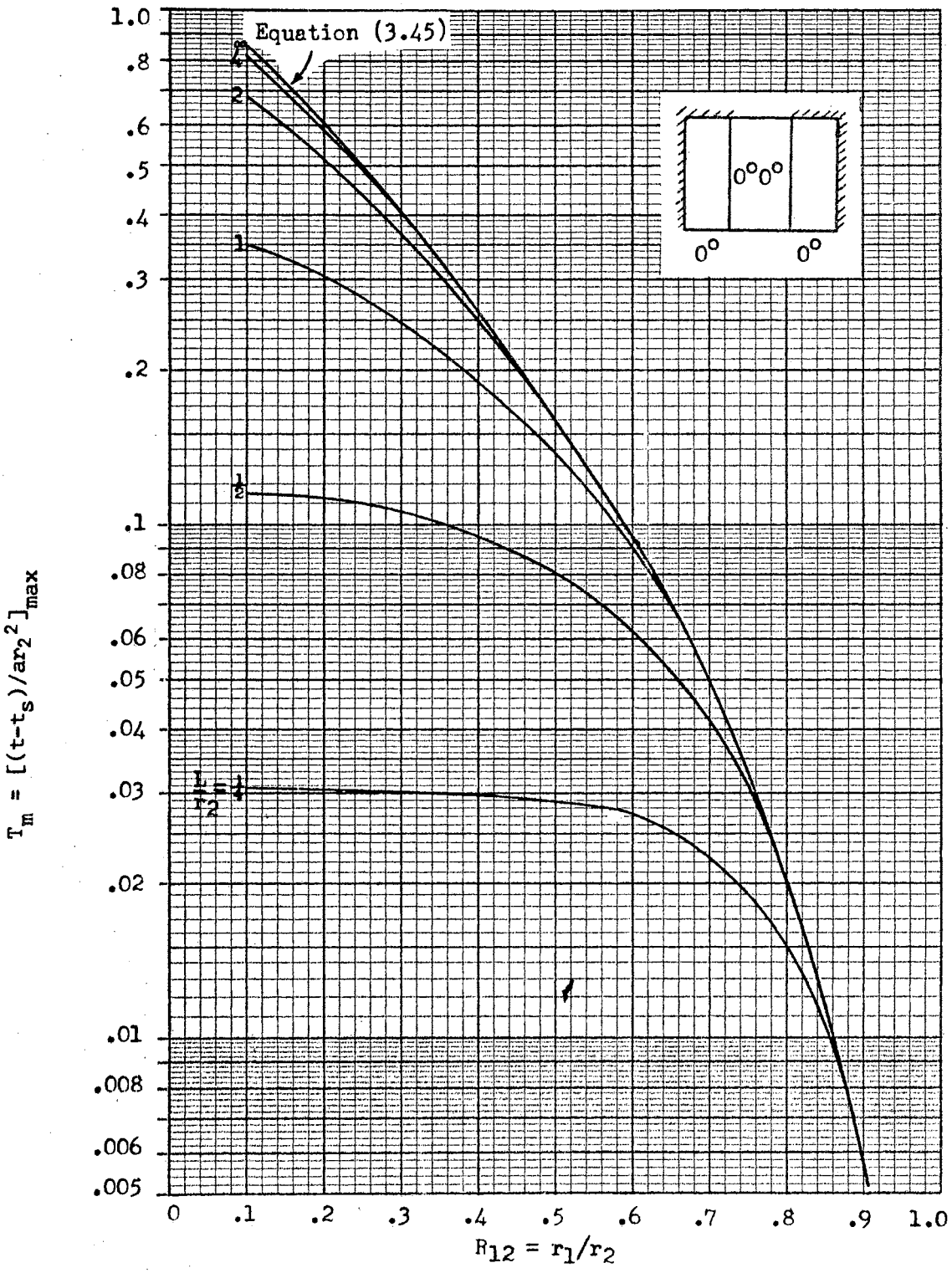

Figure 10. T_m versus R_{12} for Problems D,E, and F

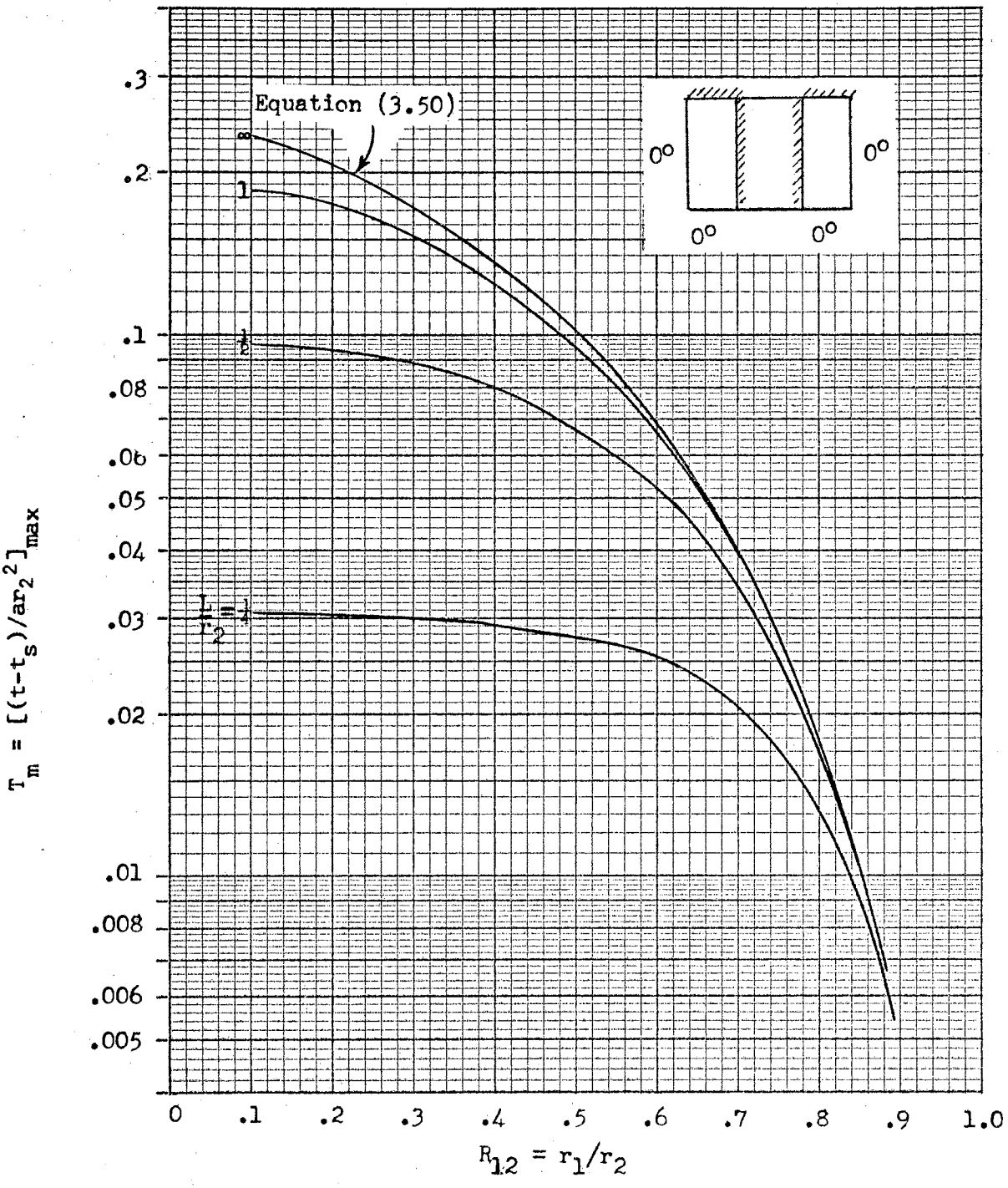

Figure 11. T_m versus R_{12} for Problems G,H, and I

as the middle curve of Figure 3 and is the solution of problem G.

The significant features of these solutions are that the effects of the curvature of the coil have not been neglected, nor have been the end effects. The results show that both effects are quite significant for coils of practical dimensions.

Use of Graphical Results

In order to determine the temperature rise within a coil, two items of information are required besides the dimensions. The first of these, and by far the easier to determine, is the heat generation per unit volume per unit time. This is easily determined by dividing the electrical power input to the coil by the volume of the coil. This gives the value of q''', first introduced in Equation 3.1.

The other bit of information required is the thermal conductivity of the composite coil. This is not so easily determined. In fact, this appears to be a research area in itself. However, some work has been done in this area.

In his book, Moore (3) presents graphically the results of a field-mapping study. Using the technique of field mapping, he generated a graph in which he relates the ratio of the thermal conductivity of the coil and that of the insulation on the coil wire to the space factor to which the coil is wound. This graph is reproduced here as Figure 12. Using the graph, a value of the conductance ratio, which is defined as the ratio of the thermal conductivity of the coil to the thermal conductivity of the insulation, is obtained for a given value of the space factor of the coil. The space factor is defined as the ratio of the volume of the copper in the coil to the entire coil volume. The thermal

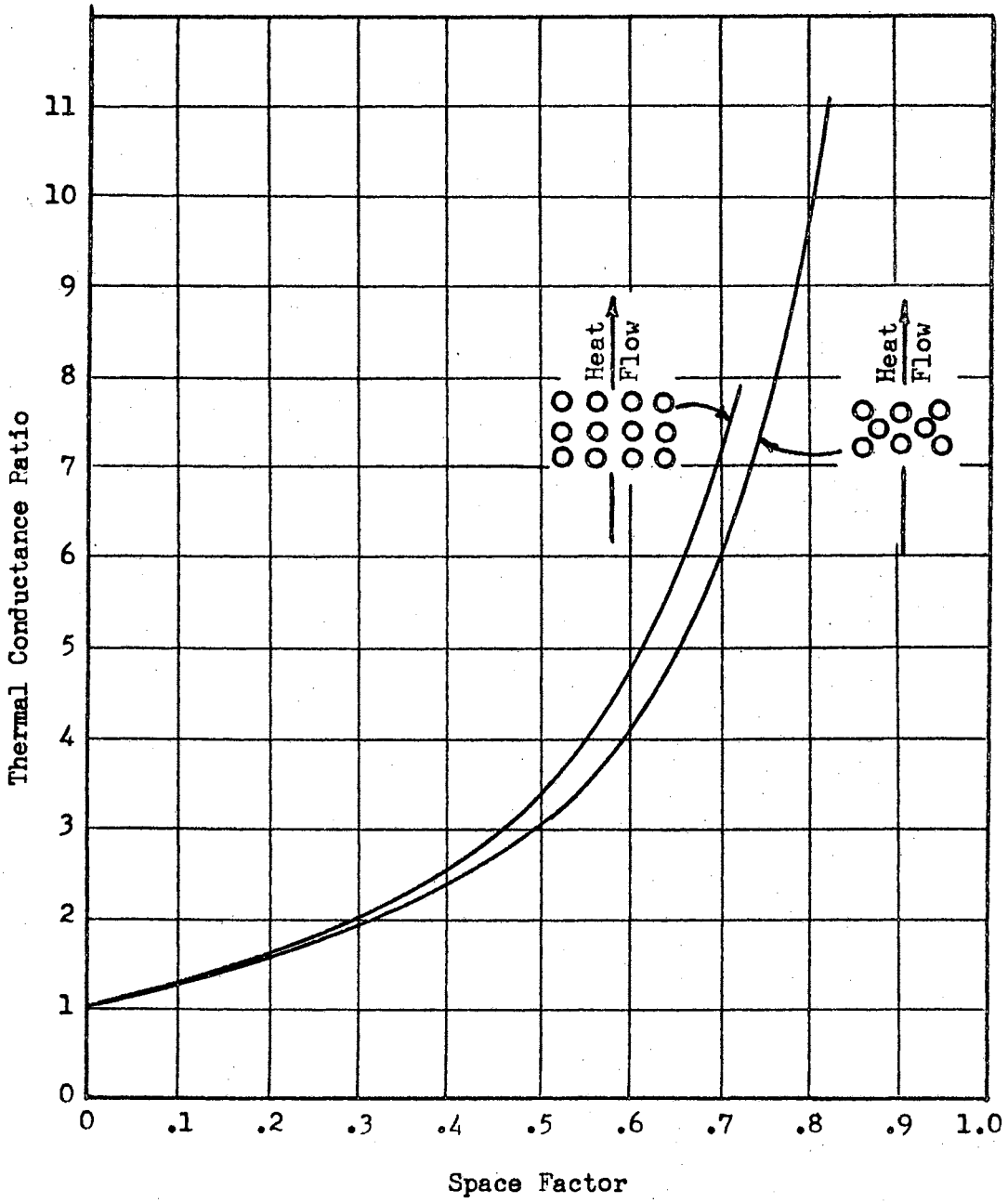

Figure 12. Thermal Conductance Ratio versus Space Factor

conductivity of the coil is given by the product of the conductance ratio and the thermal conductivity of the coil wire insulation.

Moore's work in this area has been the subject of many references, but there is very little evidence to indicate that his results have been confirmed, disputed, or extended.

After q''' and k have been determined, the use of Figures 5, 9, 10, and 11 to determine hot-spot temperature rises is a simple matter. The actual value of the temperature rise which serves as an upper bound is given by taking the product of T_m and ar_2^2, where T_m is taken from the appropriate curve of Figure 9, 10, or 11 for the proper value of R_{12} and L/r_2. As defined previously, $a = q'''/k$.

In the next chapter an example is considered in order to demonstrate the use of the graphical results of Figures 9, 10, and 12.

CHAPTER V

APPLICATION OF THE GRAPHICAL RESULTS

The coil selected to serve as an example to demonstrate the use of Figures 9, 10, and 12 is the magnet coil of a rotary-type electromagnetic relay. The iron core is stationary and serves as the major path for the heat flow out of the coil. The coil-core assembly cross section is depicted in Figure 13.

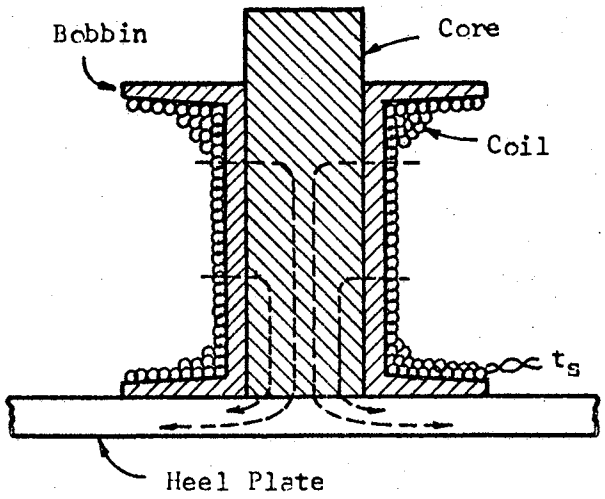

Figure 13. Coil-Core Assembly of Rotary-Type Relay

Because of the configuration of the magnetic circuit, there is no conduction path for any appreciable amount of heat flow away from the

top of the core or the top of the coil to the heat sink. Also, the proper conditions do not prevail for any significant amount of convective heat loss from the outer surface of the coil. Therefore, both the top and the outside surfaces of the coil are assumed to be adiabatic, or nearly so. With this information available, the appropriate family of curves is seen to be that of Figure 10.

The next step is to select the reference temperature, the maximum temperature occurring on the non-adiabatic portions of the coil surface. Consideration of the heat source-sink relationship indicates that the temperature increases with increasing distance from the sink. The point on the non-adiabatic portion of the surface which is furthermost from the iron core is the point (r_2, L) [See Figure 1(A)]. Therefore, the reference temperature is selected to be

$$t_s = t(r_2, L) \quad .$$

For the coil under consideration, the specifications are:

power input	8.8 watts = 30 Btu/hr.
length	0.68 in. = .0566 ft.
inner radius	0.35 in. = .0292 ft.
outer radius	0.625 in. = .052 ft.
insulation on wire	teflon
embedded winding	
reference temperature	100°F

For a space factor of 0.6, the conductance ratio for the embedded coil winding is found to be 4.1 from Figure 12. Since the thermal conductivity of teflon is approximately 0.14 Btu/hr.-ft.-°F, the

equivalent thermal conductivity of the coil is 0.57 Btu/hr.-ft.-°F.

The rate of heat generation per unit volume is determined to be

$$q''' = \frac{30 \text{ Btu/hr.}}{(r_2^2 - r_1^2)L \text{ ft.}^3} = \frac{30}{.000295} \cdot \frac{\text{Btu/hr.}}{\text{ft.}^3}$$

$$= 10.2 \times 10^4 \frac{\text{Btu/hr.}}{\text{ft.}^3} .$$

Therefore,

$$a = \frac{q'''}{k} = \frac{10.2 \times 10^4 \text{ Btu/hr.-ft.}^3}{0.57 \text{ Btu/hr.-ft.-°F}} = 1.78 \times 10^5 \text{ °F/ft.}^2$$

and

$$ar_2^2 = 480°F .$$

From Figure 10, for $R_{12} = .56$ and $L/r_2 = 1.08$, $T_m = 0.116$. The value of the upper bound on the temperature rise is given as

$$t - t_s = ar_2^2 T_m = (0.116)\ (480)\ °F = 55.6°F .$$

In other words, the actual hot-spot temperature in the coil is determined to be

$$t_m \leq t_s + 55.6°F$$

or

$$t_m \leq 100 + 55.6°F = 155.6°F .$$

If the boundary conditions of the actual coil were exactly those

shown in Figure 10, the hot-spot temperature would occur at the point $(r_2, 0)$. However, quite probably, neither the top nor the outside surface of the coil is completely adiabatic. The result of this is that the hot-spot is inside the coil but near the point $(r_2, 0)$ rather than at the point $(r_2, 0)$. As a matter of interest, the temperature at the point $(r_2, 0)$ was measured and found to be 122°F. This is a rise of 22°F above t_s.

Another upper bound on the hot-spot temperature rise within this same coil may be determined by selecting a different model from Figure 2. Previously, it was assumed that both the top and the outer radial surface of the coil are adiabatic. In this instance, assume that only the top surface is adiabatic. This corresponds to model B of Figure 2, the solution of which is given in Figure 9. For this case, the reference is that at the point $(r_2, 0)$ and is equal to 122°F.

From Figure 9, for $R_{12} = 0.56$ and $L/r_2 = 1.08$, $T_m = .025$ and

$$(t - t_s) = ar_2^2 T_m = (480)\ (0.25)\ °F = 12°F\ .$$

Therefore,

$$t_m \leq (t_s + 12)\ °F = (122 + 12)\ °F = 134°F$$

or

$$t_m \leq 134°F\ .$$

The upper bound as determined by using either Figure 9 or Figure 10 is greater than the temperature measured at the point where the surface temperature most likely assumes a value very nearly its maximum. Again, by observing the nature of the coil in its application, one would expect

the hot-spot to be very near the top and near the outer curved surface of the coil.

For this particular electrical coil, the temperature was also measured at the points $(r_1, 0)$ and (r_1, L). Using the four temperatures

$$\begin{aligned} t(r_1,0) &= 88°F \qquad t(r_2,0) = 122°F \\ t(r_1,L) &= 63°F \qquad t(r_2,L) = 100°F \end{aligned} \tag{5.1}$$

a set of temperature boundary conditions is formulated keeping in mind the assumption that there is no heat flow out the top of the coil. If the reference temperature t_s is taken to be $t(r_2, L)$ as before, then the proposed set of boundary conditions has the form

$$t(r_2,z) - t_s = a_o + a_1 z + a_2 z^2 \ , \tag{5.2}$$

$$t(r_1,z) - t_s = b_o + b_1 z + b_2 z^2 \ , \tag{5.3}$$

$$t(r,L) - t_s = c_o + c_1 r + c_2 r^2 , \tag{5.4}$$

where

$$\frac{\partial t(r_1,0)}{\partial z} = \frac{\partial t(r_2,0)}{\partial z} = \frac{\partial t(r_1,L)}{\partial r} = 0 \ . \tag{5.5}$$

The first two terms of Equation 5.5 are compatible with the assumption of no heat flow out the top of the coil. The third term of that equation provides for no heat flow into the core from the very bottom of the coil. The measured difference in the temperature of these two points indicate this to be the case for this particular coil.

By applying Equations 5.1 and 5.5 to Equations 5.2, 5.3, and 5.4,

the temperature boundary conditions are determined to be

$$t(r_2,z) - t_s = 22 - 22(z/L)^2 \ , \tag{5.6}$$

$$t(r_1,z) - t_s = -12 - 25(z/L)^2 \ , \tag{5.7}$$

$$t(r,L) - t_s = -60.4 + 2.23 \times 10^4 r^2 \ . \tag{5.8}$$

These equations are used to supply boundary temperature data for the computer program. From the computer solution of the resulting boundary-value problem, T_m is found to be approximately .0482; and the location of the hot-spot is approximately (r, z) = (0.93, 0). The hot-spot temperature rise is found to be

$$t_m - t_s = (.0482)\ (ar_2^2) = (.0482)\ (480) = 23.1°F$$

or

$$t_m = 23 + 100 = 123°F$$

The actual value of the hot-spot temperature rise is seen to be less than either of the proposed upper bounds as must be the case if the results are to be valid.

In the course of obtaining T_m for this set of boundary conditions, a discrete temperature distribution similar to the one shown at the end of Appendix A is obtained. This is shown in Figure 14. (See Appendix A for a discussion of the information presented in Figure 14.) In Figure 14, one observes that the temperatures are greater inside the outer surface than on the outer surface for the upper two-thirds of the coil. That is,

$$T_6 > T_7 \ ,$$

1	2	3	4	5	6	7
.00000	-.00295	-.00344	-.00297	-.00180	-.00034	.00000
-.02500	.00332	.02388	.03773	.04564	.04818	.04580
8	9	10	11	12	13	14
.00000	-.00477	-.00536	-.00447	-.00257	-.00029	.00000
-.02640	.00184	.02239	.03626	.04418	.04675	.04440
15	16	17	18	19	20	21
.00000	-.00404	-.00450	-.00374	-.00213	-.00022	.00000
-.03160	-.00294	.01781	.03180	.03983	.04243	.04000
22	23	24	25	26	27	28
.00000	-.00314	-.00347	-.00286	-.00161	-.00015	.00000
-.03800	-.00999	.01048	.02452	.03287	.03604	.03440
29	30	31	32	33	34	35
.00000	-.00207	-.00226	-.00184	-.00102	-.00007	.00000
-.04800	-.02118	-.00138	.01263	.02160	.02583	.02540
36	37	38	39	40	41	42
.00000	-.00094	-.00100	-.00079	-.00042	.00000	.00000
-.06100	-.03900	-.02163	-.00782	.00288	.01036	.01400
43	44	45	46	47	48	49
.00000	.00000	.00000	.00000	.00000	.00000	.00000
-.07700	-.07540	-.06290	-.04920	-.03370	-.01710	.00000

Figure 14. Discrete Temperature Distribution for the Electrical Coil of the Example (See Appendix A)

$$T_{13} > T_{14} ,$$

$$T_{20} > T_{21} ,$$

$$T_{27} > T_{28} ,$$

and

$$T_{34} > T_{35} .$$

Therefore, there is some heat flow across the outer surface. This accounts for the difference between the upper bound and the actual value of the hot-spot temperature rise. Had there been no heat flow across the outer surface, one would expect the upper bound and the actual value to be very nearly equal. This is expected because the boundary conditions used to determine the upper bound are precisely those of no heat flow across the top or the outside surfaces.

The two cases considered here for the same coil have illustrated the use of Figures 9, 10, and 12. With a minimum amount of quantitative data along with some qualitative information and a very few arithmetical operations, some knowledge of the hot-spot temperature rise within the heat-generating, hollow cylinder is easily obtained. The fact that this information is easily derived from the graphs and specifications of the coil is important to the practicing engineer when he seeks this particular type of information.

CHAPTER VI

SUMMARY AND CONCLUSIONS

Summary

In keeping with the objectives set forth in Chapter I, a method has been developed whereby certain information regarding the temperature rise in hollow, cylindrical bodies with internal heat generation may be rather easily obtained. Since the hot-spot temperature is the temperature of interest to those concerned with the possibility of component failure due to excessive internal temperatures, information that may be used to determine an upper bound on the hot-spot temperature rise is derived and presented. This information is presented graphically in a manner so as to relate the geometrical, electrical, and thermal properties of the coil to the temperature rise within the coil for a given electrical power input.

The use of the graphical relationships of Figures 9, 10, and 11 require a few rather simply determined bits of data:

1. A qualitative observation must be made of the coil in its operating environment to determine which of the coil surfaces, if any, are approximately adiabatic.
2. After the adiabatic surfaces have been noted, the location of the maximum temperature occurring on the non-adiabatic portions of the surface needs to be noted and the temperature at that

point measured or estimated, as this is the reference temperature above which the hot-spot temperature rise is determined.

3. Using the results of step 1 above and the dimensions of the coil, the appropriate curve is selected from Figure 9, 10, or 11. The value of T_m is determined.

4. From Figure 12, the "equivalent" thermal conductivity of the coil is determined to allow the calculation of the dimensional scale factor ar_2^2. Now the upper bound on the temperature rise is determined to be $t - t_s = ar_2^2 T_m$.

Conclusions

The significant conclusions are that quantitative knowledge of the hot-spot temperature rise within the cylindrical body may be derived from certain qualitative observations and a few properties of the heat-generating body; and, perhaps equally important, this knowledge may be obtained relatively easily and only a small amount of time is required. Often, in mind of the practicing engineer, the determining factor concerning the utility of a given method is the amount of time and effort required to work the method rather than the quality of the results if he has some idea of the errors involved.

The method presented is easily carried out, and the solutions presented are shown to be accurate to within five percent or better, which often is quite sufficient for engineering purposes.

The results are based on the following assumptions:

1. The thermal and electrical properties of the heat-generating body are temperature independent (including the heat generation).

2. If the results are applied to electrical coils, the assumption is made that the nonhomogeneous coil may be replaced by some homogeneous material which has the same gross thermal and electrical properties as the actual coil.

In view of some of the assumptions that have been made in prior efforts, a significant characteristic of the results is that they take full account of the effects of the curvature of the hollow cylinder as well as the end effects. Therefore, the results are valid for a right-circular, hollow cylinder of any dimension.

Areas for Future Work

One very important factor in the successful application of the results derived and presented is the determination of k, the "equivalent" thermal conductivity of the coil. The calculated value of the temperature rise varies inversely with k. Therefore, an error in the value of k affects the calculated result quite significantly. As mentioned earlier, the work of Moore (3) in this area has been referenced many times; however, there is little evidence that anyone else has looked into this problem. In view of its importance in the application of the results presented here, it seems that the problem warrants some more attention.

For certain applications of electrical coils, the maximum temperature of the non-adiabatic portion of the coil surface may not be easily determined or the point where it occurs may not be readily accessible. In these instances, it might prove desirable, for example, to be able to select some point in the magnetic circuit as the reference point or perhaps some point in the coil-mounting structure. In such cases, the

thermal conductances from the coil surfaces to the iron core or the mounting structure must be determined. Once these have been determined, perhaps the reference point may be moved to that more accessible point.

The author is presently attempting to determine these thermal conductances for the case of magnet coils where the iron core is stationary. The reference temperature is taken to be the temperature at some point in the core. In a further step, the reference point may be moved to some point in the external part of the magnetic circuit, but this requires the determination of still more conductances. More needs to be done along this line.

A SELECTED BIBLIOGRAPHY

1. Rice, L. A. "The Application of Basic Heat Transfer Principles in Optimizing Relay Design." Tenth National Conference on Electromagnetic Relays, Oklahoma State University (April, 1962).

2. Peek, R. L., Jr. and H. N. Wagar. Switching Relay Design. D. Van Nostrand Company, Inc. (1955), p. 148.

3. Moore, A. D. Fundamentals of Electrical Design. McGraw-Hill Book Company, New York (1927), pp. 96, 97.

4. Jakob, M. "Influence of Nonuniform Development of Heat Upon the Temperature Distribution in Electrical Coils and Similar Heat Sources of Simple Form." American Society of Mechanical Engineers, Transactions, Volume 65 (August, 1943), pp. 593-602.

5. Higgins, T. J. "Formulas for Calculating the Temperature Distribution in Electrical Coils of General Rectangular Cross Section." American Society of Mechanical Engineers, Transactions, Volume 66 (November, 1944), pp. 665-669.

6. Jakob, M. "Temperature Distribution in Some Simple Bodies Developing or Absorbing Heat at a Linear Function of Temperature," American Society of Mechanical Engineers, Transactions, Volume 70 (January, 1948), pp. 25-28.

7. Emmerick, C. L. "Steady-State Internal Temperature Rise in Magnet Coil Windings." Journal of Applied Physics, Volume 21 (February, 1950), pp. 75-80.

8. Peek, R. L., Jr. "Internal Temperatures of Relay Windings." Bell System Technical Journal, Volume 30 (January, 1951), pp. 141-148.

9. Peek, R. L., Jr. and H. N. Wagar. Switching Relay Design. D. Van Nostrand Company, Inc. (1955), pp. 433-439.

10. Hellums, J. D. and S. W. Churchill. "Dimensional Analysis and Natural Convection." Heat Transfer-Chemical Engineering Progress Symposium Series, No. 32, Volume 57, p. 75.

11. Peek, R. L., Jr. and H. N. Wagar. Switching Relay Design. D. Van Nostrand Company, Inc. (1955), p. 445.

12. Schneider, P. J. Conduction Heat Transfer. Addison-Wesley Publishing Company (1955), Chapter 7.

13. Dusinberre, G. M. Numerical Analysis of Heat Flow. McGraw-Hill Book Company, 1949.

14. Dusinberre, G. M. Heat Transfer Calculations by Finite Differences. International Textbook Company, 1961.

APPENDIX A

DIGITAL COMPUTER PROGRAM

The digital computer program developed and used during this study is written in Fortran IV, for use on the IBM 1410 and IBM 7090 Data Processing Systems. The discussion of this program is prefaced with the remark that no particular effort has been put forth to minimize either the execution time or the required number of memory locations of the program. On the other hand, some time was spent in developing and testing the portion of the program which examines the temperature at each node to determine whether or not it is sufficiently accurate. More is said about this later in this section.

As pointed out in Chapter IV, by using the finite-difference approximation to the differential equation, a system of linear, algebraic equations is generated. There is one equation for each node in the array. Each of the equations may be written in the form of Equation 4.1 or 4.4. Actually, both forms are used during the execution of the program. This system of equations must be solved simultaneously, since the equation for the temperature at one node involves the temperatures of several other nodes.

The simultaneous solution of the set of equations is accomplished by an iterative process. The solution is started by calculating a new value for T_1 using assumed values for all other temperatures. This new value for T_1 replaces the originally assumed value in memory and is

used in subsequent calculations. The procedure is repeated for T_2, then T_3, and so on, until a new and improved value for each temperature is obtained. In order to improve the values still more, the entire iteration process is repeated.

After some number of iterations has been completed, it is necessary to check the temperature values against some judging criterion. This is accomplished by examining the residual at each node. The residual at node 1 is defined to be the left-hand side of Equation 4.1. Just as there is a temperature equation for each node, there is a residual equation for each node. If the temperatures are all correct, the residual at each node is zero. In reality, a great many iterations may be required to reduce all residuals to zero. However, a smaller number of iterations might reduce the residuals to a value small enough that the error in the temperature values may be tolerated. This is the scheme used in the program.

After a preselected number of iterations have been completed, the residual at each node is calculated. Each of the residuals is divided by the largest value of temperature occurring after the last iteration. This provides a set of normalized residuals. If any of the normalized residuals are larger than another preselected number, another series of iterations is performed, after which the new set of normalized residuals is determined and tested. This entire process is repeated until each of the resulting normalized residuals is sufficiently small.

The iterative solution is started by using assumed values for the temperature. These assumed values are read in as data. Obviously, the closer the assumed values are to the correct values, the fewer will be the required number of iterations to yield answers correct to within a

given percentage.

The process just described is simply a variation of the method of relaxation that is explained by Schneider (12) and in detail by Dusinberre (13).

In obtaining the solutions presented in this thesis, ten iterations were performed between each examination of the normalized residuals; and the iterations were continued until every normalized residual was less than 0.01. Comments concerning the errors in these solutions are given in Appendix B.

A flow diagram of the program is given, followed by the Fortran listing and a sample of the output obtained after the residual criterion has been satisfied.

Figure 15 depicts the node array and shows the location of each of the conductances. The group of nodes which are all connected together with the dashed lines is labeled as node 50. This is the node of very high temperature mentioned in the derivation of Equation 4.3. The heat generation associated with a given node in the array is given by the product of T_{50} and the thermal conductance between node 50 and that node. For example, the heat generation associated with node 1 is

$$Q_{g1} = K_{110}T_{50} .$$

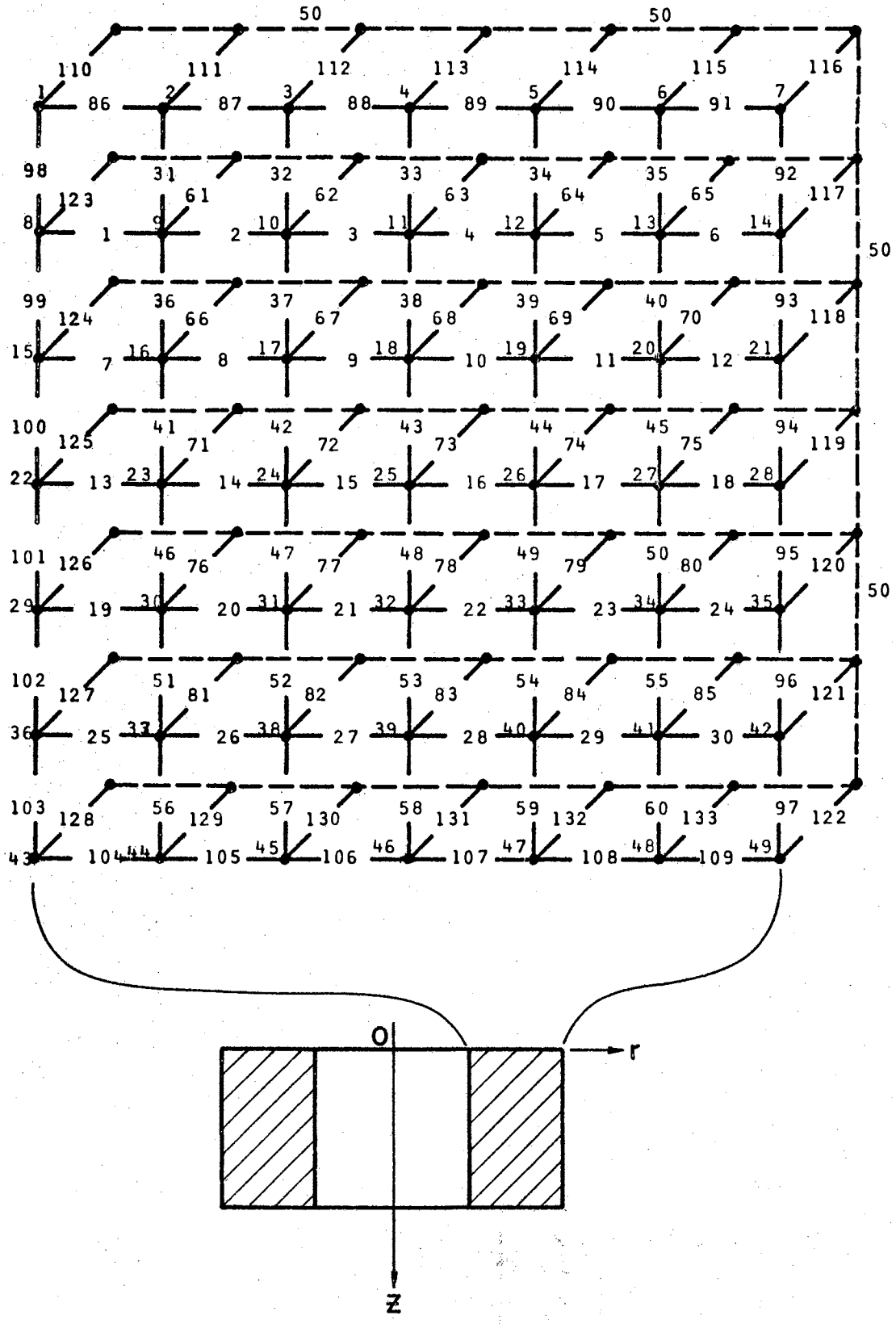

Figure 15. Node Array Showing Location of Each Conductance

Flow Diagram:

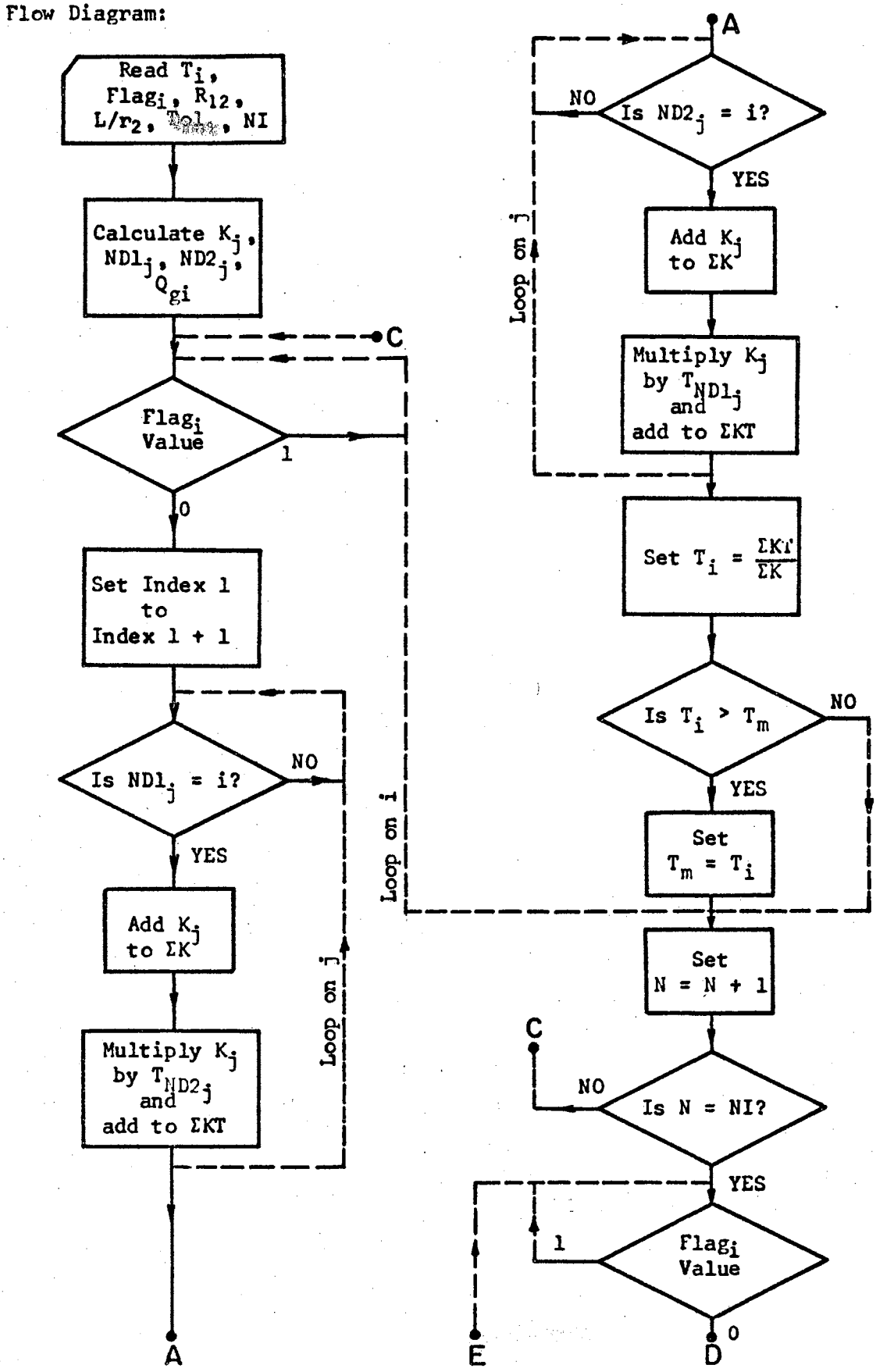

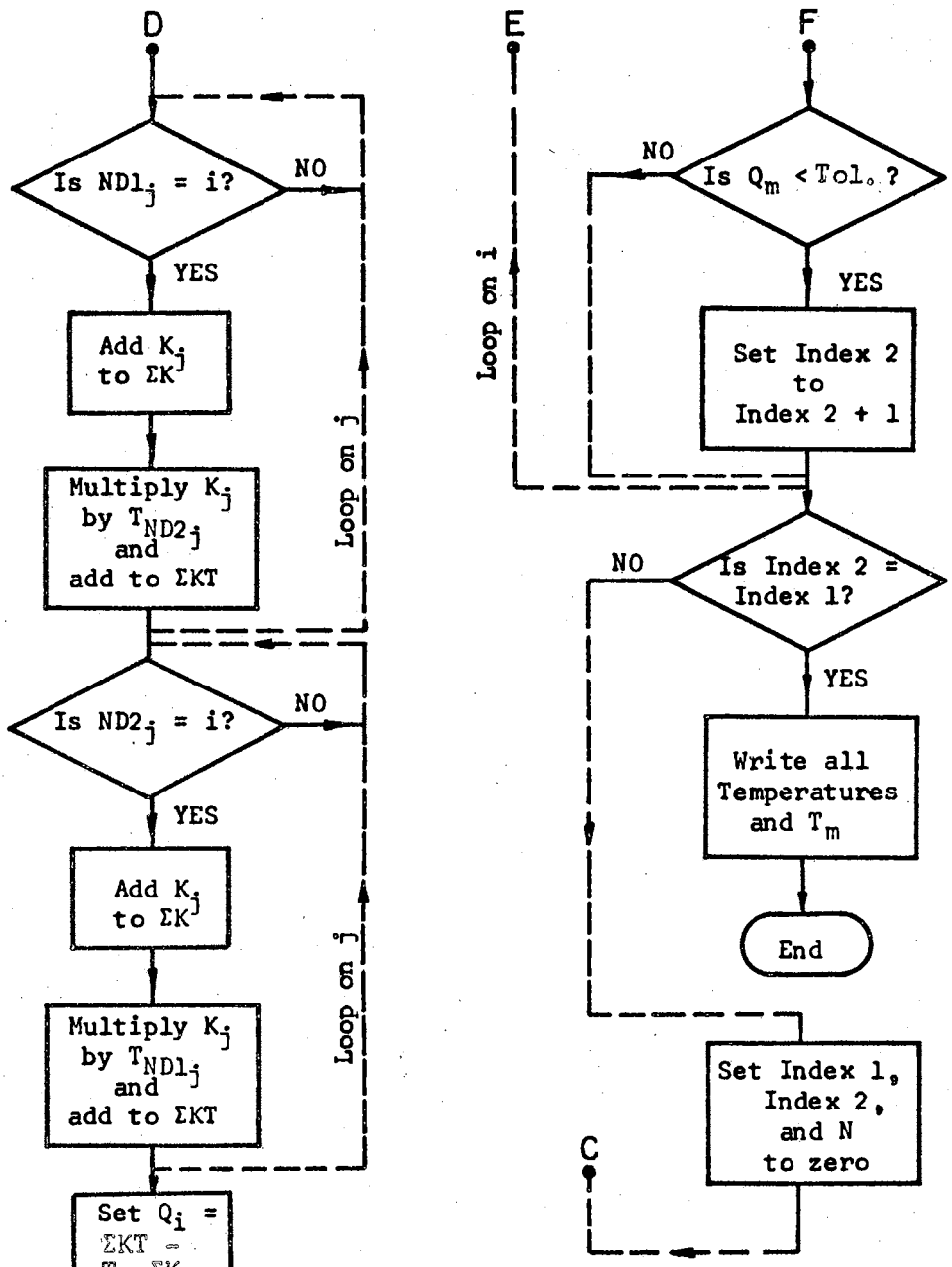

Notation:

$Flag_i$ = 0 an active node

$Flag_i$ = 1 a boundary node

Tol. - the largest value of residual allowed after final iteration

NI - the number of iterations between each residual test

$ND1_j$, $ND2_j$ - nodes associated with conductance K_j

```
      DIMENSION T(100),IFLAG(100),TK(150),ND1(150),ND2(150),V(25)
      DIMENSION RHO(25),QN(100)
1000  FORMAT(I10,I10,F10.5)
2000  FORMAT(F10.5,I10)
3000  FORMAT(1H1,9X,12HRUNNING TIME,5X,F7.3,5X,5HHOURS,//)
3500  FORMAT(10X,20HNUMBER OF ITERATIONS,5X,I10,//)
4000  FORMAT(10X,14HRATIO OF INNER,5X,15HRATIO OF LENGTH)
5000  FORMAT(10X,15HTO OUTER RADIUS,4X,15HTO OUTER RADIUS,/)
6000  FORMAT(F10.5)
7000  FORMAT(13X,F7.3,12X,F7.3,//)
7500  FORMAT(10X,31HTHE TEMPERATURE DISTRIBUTION IS,//)
8000  FORMAT(12X,I2,6(11X,I2))
8500  FORMAT(3X,7(3X,F10.5))
9000  FORMAT(3X,7(3X,F10.5),//)
9500  FORMAT(10X,22HMAXIMUM TEMPERATURE IS,5X,F10.5,5X,7HAT NODE,5X,I2)
9600  FORMAT(10X,48HWHERE THE NUMBERS ARE NODE, NORMALIZED RESIDUAL,)
9700  FORMAT(10X,43HAND DIMENSIONLESS TEMPERATURE, RESPECTIVELY)
      CALL CLOCK (STTIME)
      N=1
      NN=1
1     ITERAT=0
      ICOUNT=0
      ICMAX=10
      IIN=1
      IOUT=3
      READ(IIN,1000)IMAX,JMAX,TOL
      READ(IIN,6000)RB
      READ(IIN,6000)ZB
      PI=3.141592
      IND1=0
      IND2=0
100   DO 105 I=1,IMAX
105   READ(IIN,2000)T(I),IFLAG(I)
5     DELTR=(1.0-RB)/6.0
      RHO(1)=RB
      DO 10 I=2,7
      RHO(I)=RHO(I-1)+DELTR
10    CONTINUE
15    DELTL=ZB/6.0
      DO 20 I=1,6
      TK(I)=2.0*PI*DELTL/ALOG(1.0+DELTR/RHO(I))
      ND1(I)=I+7
      ND2(I)=I+8
20    CONTINUE
      DO 25 I=1,24
      TK(I+6)=TK(I)
      ND1(I+6)=ND1(I)+7
      ND2(I+6)=ND2(I)+7
25    CONTINUE
      DO 30 I=2,6
      TK(I+29)=2.0*PI*RHO(I)*DELTR/DELTL
      ND1(I+29)=I
      ND2(I+29)=I+7
      V(I+7)=2.0*PI*DELTR*DELTL*RHO(I)
30    CONTINUE
      DO 35 I=31,55
      TK(I+5)=TK(I)
      ND1(I+5)=ND1(I)+7
      ND2(I+5)=ND2(I)+7
35    CONTINUE
      DO 40 I=9,13
      TK(I+52)=V(I)/100000.0
```

```
      ND1(I+52)=I
      ND2(I+52)=50
40    CONTINUE
      DO 45 I=61,80
      TK(I+5)=TK(I)
      ND1(I+5)=ND1(I)+7
      ND2(I+5)=50
45    CONTINUE
      DO 50 I=1,6
      TK(I+85)=TK(I)/2.0
      ND1(I+85)=I
      ND2(I+85)=I+1
      TK(I+103)=TK(I+85)
      ND1(I+103)=I+42
      ND2(I+103)=I+43
50    CONTINUE
      TK(92)=PI*(RHO(7)*DELTR-(DELTR**2)/4.0)/DELTL
      ND1(92)=7
      ND2(92)=14
      DO 55 I=1,5
      TK(I+92)=TK(92)
      ND1(I+92)=7*(I+1)
      ND2(I+92)=7*(I+2)
55    CONTINUE
      TK(98)=PI*(RHO(1)*DELTR+(DELTR**2)/4.0)/DELTL
      ND1(98)=1
      ND2(98)=8
      DO 60 I=1,5
      TK(I+98)=TK(98)
      ND1(I+98)=7*I+1
      ND2(I+98)=7*I+8
60    CONTINUE
      VOL=PI*DELTL*(RHO(1)*DELTR+(DELTR**2)/4.0)
      TK(123)=VOL/100000.0
      ND1(123)=8
      ND2(123)=50
      DO 65 I=1,4
      TK(I+123)=TK(123)
      ND1(I+123)=7*I+8
      ND2(I+123)=50
65    CONTINUE
      TK(110)=TK(123)/2.0
      ND1(110)=1
      ND2(110)=50
      TK(128)=TK(110)
      ND1(128)=43
      ND2(128)=50
      DO 70 I=1,5
      TK(I+110)=TK(I+60)/2.0
      ND1(I+110)=I+1
      ND2(I+110)=50
      TK(I+128)=TK(I+110)
      ND1(I+128)=I+43
      ND2(I+128)=50
70    CONTINUE
      VOL=PI*DELTL*(RHO(7)*DELTR-(DELTR**2)/4.0)
      TK(117)=VOL/100000.0
      ND1(117)=14
      ND2(117)=50
      DO 75 I=1,4
      TK(I+117)=TK(117)
      ND1(I+117)=7*I+14
```

```
      ND2(I+117)=50
75    CONTINUE
      TK(116)=TK(117)/2.0
      ND1(116)=7
      ND2(116)=50
      TK(122)=TK(116)
      ND1(122)=49
      ND2(122)=50
119   TMAX=0.0
120   DO 225 I=1,IMAX
      SUMK=0.0
      SUMKT=0.0
      IF(IFLAG(I).EQ.1)GO TO 225
      DO 156 J=1,JMAX
      IF(ND1(J).NE.I)GO TO 156
      SUMK=SUMK+TK(J)
      M=ND2(J)
      SUMKT=SUMKT+TK(J)*T(M)
156   CONTINUE
      DO 182 J=1,JMAX
      IF(ND2(J).NE.I)GO TO 182
      SUMK=SUMK+TK(J)
      M=ND1(J)
      SUMKT=SUMKT+TK(J)*T(M)
182   CONTINUE
      TEMP=SUMKT/SUMK
      T(I)=TEMP
      IF(TMAX.GT.T(I))GO TO 225
      TMAX=T(I)
      NODE=I
225   CONTINUE
      ITERAT=ITERAT+1
      ICOUNT=ICOUNT+1
      IF(ICOUNT.NE.ICMAX)GO TO 119
      ICOUNT=0
      DO 245 I=1,IMAX
      SUMK=0.0
      SUMKT=0.0
      IF(IFLAG(I).EQ.1)GO TO 243
      IND1=IND1+1
      DO 227 J=1,JMAX
      IF(ND1(J).NE.I)GO TO 227
      SUMK=SUMK+TK(J)
      M=ND2(J)
      SUMKT=SUMKT+TK(J)*T(M)
227   CONTINUE
      DO 228 J=1,JMAX
      IF(ND2(J).NE.I)GO TO 228
      SUMK=SUMK+TK(J)
      M=ND1(J)
      SUMKT=SUMKT+TK(J)*T(M)
228   CONTINUE
      Q=SUMKT-T(I)*SUMK
      QN(I)=Q/TMAX
      IF(ABS(QN(I)).GE.TOL)GO TO 245
      IND2=IND2+1
      GO TO 245
243   QN(I)=0.0
245   CONTINUE
230   IF(IND1.NE.IND2)GO TO 250
      GO TO 275
250   IND1=0
```

```
      IND2=0
260   GO TO 119
275   CONTINUE
      CALL CLOCK (PRTIME)
      RNTIME=PRTIME-STTIME
      WRITE(IOUT,3000)RNTIME
      WRITE(IOUT,3500)ITERAT
      WRITE(IOUT,4000)
      WRITE(IOUT,5000)
      WRITE(IOUT,7000)RB,ZB
      WRITE(IOUT,7500)
      DO 244 L=1,43,7
      L1=L
      L2=L+1
      L3=L+2
      L4=L+3
      L5=L+4
      L6=L+5
      L7=L+6
      WRITE(IOUT,8000)L1,L2,L3,L4,L5,L6,L7
      WRITE(IOUT,8500)QN(L1),QN(L2),QN(L3),QN(L4),QN(L5),QN(L6),QN(L7)
      WRITE(IOUT,9000)T(L1),T(L2),T(L3),T(L4),T(L5),T(L6),T(L7)
244   CONTINUE
      WRITE(IOUT,9500)TMAX,NODE
      WRITE(IOUT,9600)
      WRITE(IOUT,9700)
246   CONTINUE
      ITERAT=0
      IF(RNTIME.GT.0.8)GO TO 291
      RB=RB+0.125
      IF(RB.GT.0.90)GO TO 280
      GO TO 5
280   RB=0.125
      ZB=2.0*ZB
      IF(ZB.GT.5.0)GO TO 290
      GO TO 5
290   ZB=0.25
291   CONTINUE
295   STOP
      END
```

RUNNING TIME .190 HOURS

NUMBER OF ITERATIONS 30

RATIO OF INNER TO OUTER RADIUS	RATIO OF LENGTH TO OUTER RADIUS
.250	4.000

THE TEMPERATURE DISTRIBUTION IS

1	2	3	4	5	6	7
.00000	-.00090	-.00106	-.00092	-.00052	-.00003	.00000
.00000	.04903	.07033	.07290	.06075	.03602	.00000
8	9	10	11	12	13	14
.00000	-.00162	-.00190	-.00162	-.00091	-.00003	.00000
.00000	.04903	.07033	.07290	.06075	.03602	.00000
15	16	17	18	19	20	21
.00000	-.00157	-.00183	-.00156	-.00088	-.00002	.00000
.00000	.04903	.07032	.07289	.06074	.03602	.00000
22	23	24	25	26	27	28
.00000	-.00150	-.00175	-.00149	-.00083	-.00002	.00000
.00000	.04897	.07024	.07280	.06067	.03598	.00000
29	30	31	32	33	34	35
.00000	-.00129	-.00149	-.00126	-.00070	-.00001	.00000
.00000	.04845	.06946	.07201	.06004	.03564	.00000
36	37	38	39	40	41	42
.00000	-.00076	-.00087	-.00072	-.00039	.00000	.00000
.00000	.04373	.06245	.06477	.05425	.03249	.00000
43	44	45	46	47	48	49
.00000	.00000	.00000	.00000	.00000	.00000	.00000
.00000	.00000	.00000	.00000	.00000	.00000	.00000

MAXIMUM TEMPERATURE IS .07290 AT NODE 4
WHERE THE NUMBERS ARE NODE, NORMALIZED RESIDUAL,
AND DIMENSIONLESS TEMPERATURE, RESPECTIVELY

APPENDIX B

ERROR ANALYSIS OF APPROXIMATE SOLUTIONS

The error analysis given here is to provide a feel for the magnitude of the errors involved in the solutions described in Chapter IV. Recalling that those solutions were obtained by solving a finite-difference model which is only an approximation to the original mathematical model. There is, therefore, an error involved due to the finite difference approximation. Secondly, the approximate model is solved by an iteration technique which provides another source of error. The iteration process may be continued as long as practicable, but the resulting solution only converges toward the correct solution to the model and, in general, never becomes equal to it. Thirdly, there is error introduced into the solution due to round-off and truncation which take place during the actual computing process. Therefore, there are at least three sources of error:

1. Error due to the finite difference approximation,
2. Error due to convergence characteristics of the programmed solution,
3. Error due to round-off and truncation occurring during the computing process.

Some idea of the magnitude of the error due to the finite difference approximation may be obtained by considering the mathematics of that numerical method. Consider the case where the dimensionless temperature

T is a function only of the dimensionless radial variable R. That is, T(R) must satisfy Equation 3.28,

$$\frac{d^2T}{dR^2} + \frac{1}{R} \cdot \frac{dT}{dT} + 1 = 0 \ . \qquad (3.28)$$

If T(R) is expressed in a Taylor series expansion in the following manner, an indication of the magnitude of error is obtained.

$$T(R + \Delta R) = T(R) + \Delta R \frac{dT(R)}{dR} + \frac{(\Delta R)^2}{2} \cdot \frac{d^2T(R)}{dR^2}$$

$$+ \frac{(\Delta R)^3}{3!} \cdot \frac{d^3T(R)}{dR^3} + \frac{(\Delta R)^4}{4!} \cdot \frac{d^4T(R)}{dT^4} + \ldots \qquad (B.1)$$

$$T(R - \Delta R) = T(R) - \Delta R \frac{dT(R)}{dR} + \frac{(\Delta R)^2}{2} \cdot \frac{d^2T(R)}{dR^2}$$

$$- \frac{(\Delta R)^3}{3!} \cdot \frac{d^3T(R)}{dR^3} + \frac{(\Delta R)^4}{4!} \cdot \frac{d^4T(R)}{dR^4} + \ldots \qquad (B.2)$$

Upon adding Equations B.1 and B.2 together and solving for $\frac{d^2T(R)}{dR^2}$, one obtains

$$\frac{d^2T(R)}{dR^2} = \frac{1}{(\Delta R)^2} [T(R + \Delta R) + T(R - \Delta R) - 2T(R) + o(\Delta R)^4] \ , \qquad (B.3)$$

or

$$\frac{d^2T(R)}{dR^2} = \frac{1}{(\Delta R)^2} [T(R + \Delta R) + T(R - \Delta R) - 2T(R)] + o(\Delta R)^2 \ . \qquad (B.4)$$

Therefore, if only the first three terms of the series expansion are

considered, the error is of order $(\Delta R)^2$. Similarly,

$$\frac{dT(R)}{dR} = \frac{T(R + \Delta R) - T(R - \Delta R)}{2\ \Delta R} + o(\Delta R)^2 \quad . \tag{B.5}$$

If the right-hand side of Equations B.4 and B.5 are substituted into Equation 3.28, the result is

$$\frac{d^2T(R)}{dR^2} + \frac{1}{R} \cdot \frac{dT(R)}{dR} = \frac{1}{(\Delta R)^2} [T(R + \Delta R) + T(R - \Delta R) - 2T(R)]$$

$$+ \frac{1}{2\ R} [T(R + \Delta R) - T(R - \Delta R)] + o(\Delta R)^2 = -1 \ , \tag{B.6}$$

which gives the correct solution if the term $o(\Delta R)^2$ can be evaluated. The central difference numerical approximation neglects this term; and, therefore, it is the error due to the approximation.

Equations 4.1 and 4.4 may be generated from Equation B.6 which serves as the basis for the calculation of temperature distribution by finite-differences.

From Equation 4.7

$$\Delta R = \frac{1 - R_{12}}{6} \tag{4.7}$$

Therefore,

$$(\Delta R)^2 = (1 - 2R_{12} + R_{12}^2)/36 \ . \tag{B.7}$$

Equation B.7 is evaluated for values of R_{12} between zero and one as follows:

R_{12}	$(\Delta R)^2$	
0	.0278	2.78%
.1	.0225	2.25
.3	.0113	1.13
.5	.0069	0.69
.7	.0025	0.25
.9	.00028	0.028
1.0	0	0

This shows that the magnitude of the error resulting from the finite difference approximation is of the order of three percent or less.

The other two errors listed are not so easily determined. However, in certain cases, it is not difficult to determine the entire error involved. In order to do this, a boundary-value problem which is described by Equation 3.28 is selected from Figure 2. Problem D of Figure 2 is such a problem, and the solution is given by Equation 3.45. A feel for the total error involved in the approximate solution may be obtained by comparing the exact solution, Equation 3.45, with the computed solution of the finite-difference model. This comparison is shown in the table below:

R_{12}	Solution for T_m		Percent	$(\Delta R)^2$
	Exact	Computed	Error	
0.125	.79362	.75467	-4.91	2.12%
0.250	.45877	.47359	3.23	1.56
0.375	.27557	.28061	1.82	1.08
0.500	.15907	.16090	1.15	0.69
0.625	.08265	.08314	0.59	0.39
0.750	.03446	.03460	0.40	0.17
0.875	.00817	.00819	0.24	0.05

In this case, the magnitude of the actual error is roughly two times $(\Delta R)^2$ which is well within the confines of the definition of $o(\Delta R)^2$. As mentioned before, it is difficult to separate out each of the three errors to determine the contribution of each. However, the fact of importance here is that the total error involved by the approximate solution appears to be less than five percent, which is sufficiently small for many engineering purposes.

Equations similar to B.1 through B.6 may be derived for the problems where the heat flow has both radial and axial components. However, the mathematics required to determine the order of the error are a bit more complex. It is felt that this one example is sufficient to give one a feeling of the magnitudes of error involved and to assure that the solutions presented in Figures 9, 10, and 11 are sufficiently accurate for many applications.

APPENDIX C

GLOSSARY OF SYMBOLS

The following is a list of the symbols and terms used through the thesis:

- a - q'''/k (defined after Equation 3.8)
- C - specific heat
- k - thermal conductivity
- L - length of the hollow cylinder
- q''' - heat generated per unit volume per unit time
- r_1 - inner radius of the hollow cylinder
- r_2 - outer radius of the hollow cylinder
- R_{12} - the ratio r_1/r_2
- R_m - dimensionless radius at which the hot-spot temperature occurs
- $\bar{R}$ - defined in Equation 3.41
- t - dependent variable, temperature
- t_m - upper bound on t
- t_s - reference temperature
- T - dimensionless temperature differences (defined by Equations 3.9 and 3.12)
- T_m - upper bound on T
- α - thermal diffusivity
- β - temperature coefficient of resistivity

θ - independent variable, time

ρ - mass density

ρ_i - values of the dimensionless radius R (i = 1, 2, ..., 7)

VITA

Troy James Pemberton

Candidate for the Degree of

Doctor of Philosophy

Thesis: STEADY-STATE TEMPERATURE RISE IN CYLINDERS WITH INTERNAL HEAT GENERATION

Major Field: Engineering

Biographical:

Personal Data: Born at Ponca City, Oklahoma, December 18, 1937, the son of J. Hersel and Alice L. Pemberton.

Education: Graduated from Ponca City High School in 1955; attended Northern Oklahoma Junior College, Tonkawa, Oklahoma, from September, 1957, to May, 1959; transferred to Oklahoma State University, Stillwater, Oklahoma, in September, 1959; received the degrees of Bachelor of Science in 1962 and Master of Science in 1963 with a major in Electrical Engineering from the Oklahoma State University; completed requirements for the degree of Doctor of Philosophy with a major in Electrical Engineering in August, 1965.

Professional Experience: Employed part time and full time for six years as radio and television repairman, 1952-1960; employed one summer (1960) as corrosion control technician, Continental Oil Company, Ponca City, Oklahoma; employed as student assistant one semester (1962) by Oklahoma State University; employed one summer (1962) as research engineer, Texas Instruments, Incorporated, Dallas, Texas; employed one summer (1963) as research engineer, California Research Corporation, LaHabra, California; employed seventeen months (1964-1965) as research assistant, School of Electrical Engineering, Oklahoma State University.

Professional Organizations: Student member of Institute of Electrical and Electronics Engineers; Engineer-in-Training No. 1106, Mid-North Chapter, Oklahoma Society of Professional Engineers; National Society of Professional Engineers.